Astana | 12 January 2023

PhD Candidate: Iliyas Tursynbek

Design, Motion Planning, and Control of a Spherical Parallel Manipulator with Coaxial Input Shafts

Lead Supervisor: Dr. Almas Shintemirov (NU SEDS)
Internal Co-Supervisor: Dr. Matteo Rubagotti (NU SEDS)
External Co-Supervisor: Dr. Alexandr Klimchik (University of Lincoln, UK)

Introduction

Serial vs Parallel Manipulators

Advantages of PMs (usually):

- Higher payload
- Higher stiffness
- Higher precision
- Higher speed
- Lower inertia

Disadvantages of PMs:

- Small workspace
- Complicated analysis
- Complicated control

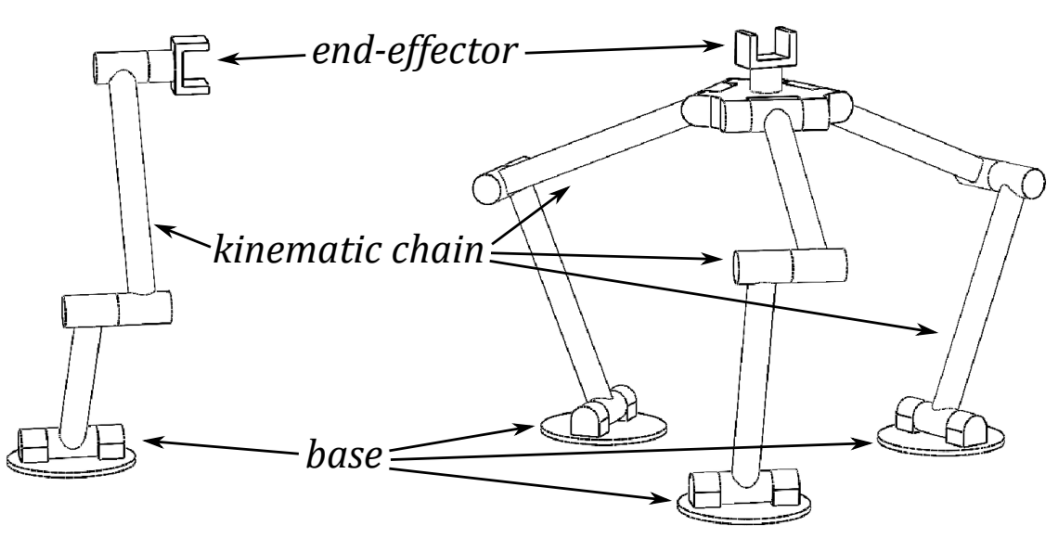

Fig. 1: Serial vs. parallel manipulators

Introduction

Types of Parallel Manipulators

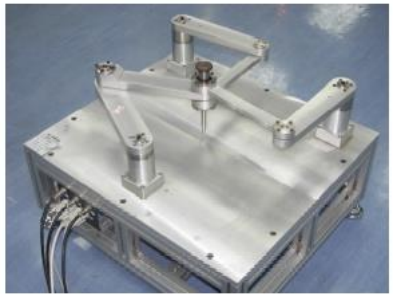

Planar PM [1] (2-3 DOF)

*source https://robot.gmc.ulaval.ca/

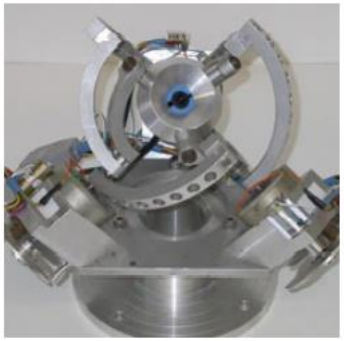

Spherical PMs (2-3 DOF)

Example: Agile Eye

*courtesy of B&R Industrial Automation GmbH

*courtesy of Physik Instrumente (PI)

Spatial PMs (3-6 DOF)

Example: Delta and Stewart-Gough

Fig. 2: Types of PMs

[1] W. Shang, S. Cong, and Y. Zhang, “Nonlinear friction compensation of a 2-dof planar parallel manipulator,” Mechatronics, vol. 18, no. 7, pp. 340–346, 2008.

Introduction

Spherical Parallel Manipulators

Spherical Parallel Manipulators (SPMs) can provide 3 pure rotational DOFs

Fig. 3: 2-axis pan-tilt platforms

Possible application as an orientation platform or robotic wrist (active ball joint)

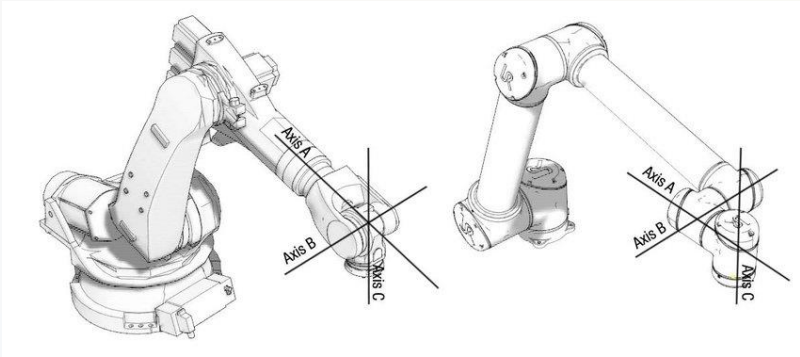

Fig. 4: Serial robotic wrists [2]

[2] K. Elashry, and R. Glynn, “An approach to automated construction using adaptive programing,” In Robotic Fabrication in Architecture, Art and Design 2014, pp. 51-66. Springer, Cham, 2014.

Introduction

Spherical Parallel Manipulators

Motion control platforms (orientation platforms) can perform at least one of the following operations:

- Object orientation
- Target tracking
- Object stabilization

Usually, a manipulator utilizing all three rotational DOFs and capable of extended roll-rotation is required. SPM is a good candidate.

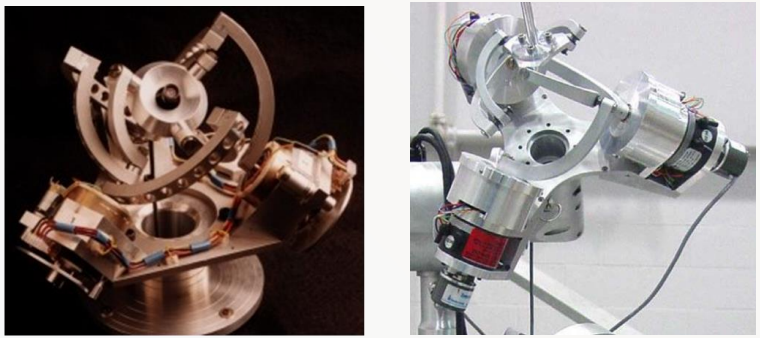

Fig. 5: SPM examples

(left – Agile Eye [3], right – Agile Wrist [4])

[3] C. M. Gosselin, E. St. Pierre, and M. Gagne, "On the development of the Agile Eye," IEEE Robotics & Automation Magazine, vol. 3, no. 4, pp. 29–37, 1996.
[4] K. Al-Widyan, X. Q. Ma, and J. Angeles, "The robust design of parallel spherical robots," Mechanism and Machine Theory, vol. 46, no. 3, pp. 335–343, 2011.

Introduction

Spherical Parallel Manipulators

Orientation platforms are important in applications such as:

- Mobile robotics
- Machining
- Humanoid robotics
- Exoskeletons
- Medical and surgical robotics

Hence, the motivation for researching SPMs.

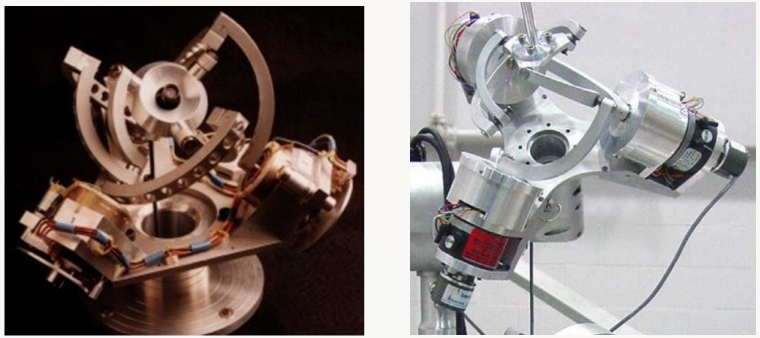

Fig. 5: SPM examples

(left – Agile Eye [3], right – Agile Wrist [4])

[3] C. M. Gosselin, E. St. Pierre, and M. Gagne, "On the development of the Agile Eye," IEEE Robotics & Automation Magazine, vol. 3, no. 4, pp. 29–37, 1996.
[4] K. Al-Widyan, X. Q. Ma, and J. Angeles, "The robust design of parallel spherical robots," Mechanism and Machine Theory, vol. 46, no. 3, pp. 335–343, 2011.

Introduction

Hypothesis, objectives, and scope of the work

Hypothesis:

Motion control platforms can be developed based on the coaxial SPM with capabilities to infinitely rotate its mobile platform and achieve target tracking and object stabilization.

Objectives:

- Studying kinematics of the developed coaxial SPM
- Studying effects of the infinite rotational motion (3rd DOF)
- Implement target tracking and object stabilization with the experimental setup

Scope of the work:

- Performing kinematic analysis
- Computing workspace and configurations space
- Integrating an external control device and inertial sensor with the experimental setup

Introduction

Background Research and Literature Review

SPMs can be classified in different ways based on their:

- Mobility (DOFs): 2-DOF, 3-DOF
- Joint type: revolute (R), cylindrical (C), universal (U), spherical (S), prismatic (P)
- Structure: number of limbs, presence of passive limbs
- Symmetry: symmetrical, asymmetrical

Most common type is a 3-DOF 3-RRR symmetrical SPM (general SPM).

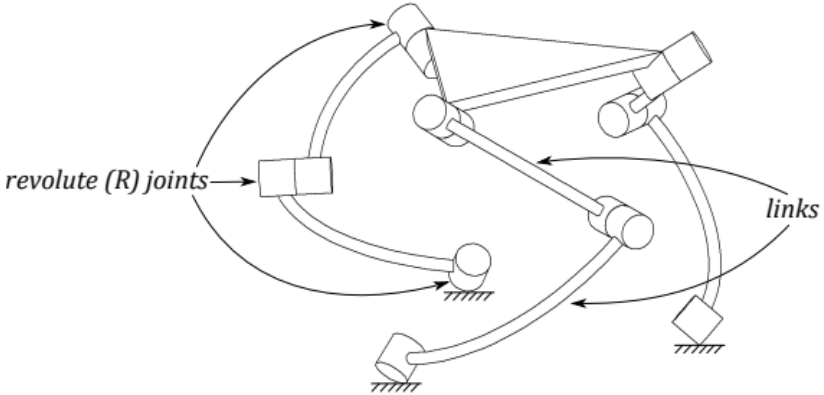

Fig. 6: Spherical parallel manipulator

Introduction

Background Research and Literature Review

- One of the earliest research works that considered a robotic wrist based on parallel kinematic architecture is by Asada and Granito (1985) [5].
- It was followed with the works by Cox (1989), Marco (1989), Craver (1989), Alizade (1994) and others focusing on parallel shoulder module [6-9].
- These PMs are of 3-RRR SPM type.

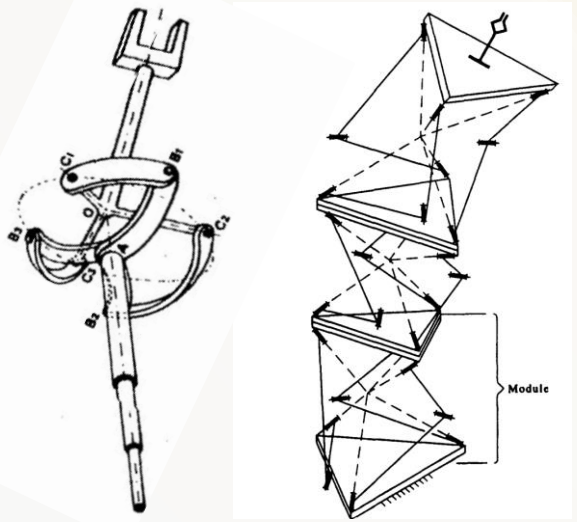

Fig. 7: Early SPM examples
(left - parallel robotic wrist by Asada and Granito,
right – stacked parallel robotic shoulder by Alizade *et al.)*

[5] H. Asada and J. Granito, "Kinematic and static characterization of wrist joints and their optimal design," in Proceedings of the 1985 IEEE International Conference on Robotics and Automation (ICRA), pp. 244–250, 1985.
[6] D. J. Cox and D. Tesar, "The dynamic model of a three degree of freedom parallel robotic shoulder module," in Advanced Robotics: 1989, pp. 475–487, Springer, 1989.
[7] D. Marco, L. Torfason, and D. Tesar, "Computer simulation and design of a three degree-of-freedom shoulder module," pp. 273–282, 1989.
[8] W. M. Craver, "Structural analysis and design of a three-degree-of-freedom robotic shoulder module," Master's thesis, University of Texas, Austin TX, 1989.
[9] R. I. Alizade, N. R. Tagiyev, and J. Duffy, "A forward and reverse displacement analysis of an in-parallel spherical manipulator," Mechanism and Machine Theory, vol. 29, no. 1, pp. 125–137, 1994.

Introduction

Background Research and Literature Review

One of the major contributions to design and analysis of SPMs was made by Gosselin *et al.*:

- Gosselin and Angeles (1989) addressed inverse kinematics of general SPMs [10].
- Gosselin *et al.* (1994) derived 8th order polynomial to solve forward kinematics of SPM with a coplanar platform [11].
- Gosselin *et al.* (1994) derived 8th order polynomial to solve forward kinematics of SPM of general architecture [12]. It was proven to be minimal.

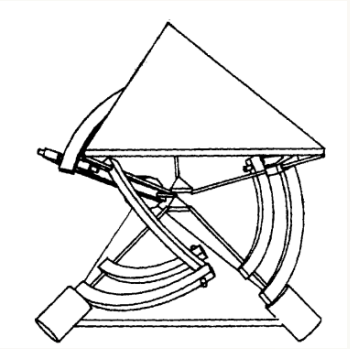

Fig. 8: General SPM [10, 12]

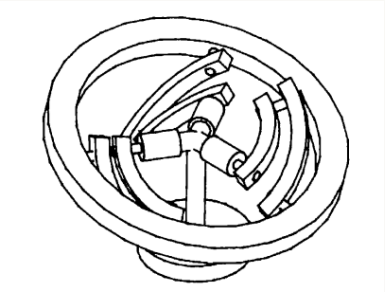

Fig. 9: Coplanar SPM [11]

[10] C. M. Gosselin and J. Angeles, "The optimum kinematic design of a spherical three-degree-of-freedom parallel manipulator," Journal of Mechanisms, Transmissions, and Automation in Design, vol. 111, no. 2, pp. 202–207, 1989.
[11] C. M. Gosselin, J. Sefrioui, and M. J. Richard, "On the direct kinematics of spherical three-degree-of-freedom parallel manipulators with a coplanar platform," Journal of Mechanical Design, vol. 116, no. 2, pp. 587–593, 1994.
[12] C. M. Gosselin, J. Sefrioui, and M. J. Richard, "On the direct kinematics of spherical three-degree-of-freedom parallel manipulators of general architecture," Journal of Mechanical Design, vol. 116, no. 2, pp. 594–598, 1994.

Introduction

Background Research and Literature Review

- Agile Eye SPM was developed by Gosselin *et al.* in 1994 [13]. It is a 3-DOF camera-orienting device. It orients a mounted camera within a cone of 140° opening with ±30° in torsion.
- In 2009, Kong and Gosselin [14] derived a formula for obtaining a unique solution to the forward kinematic problem corresponding to its working and assembly mode.
- An enhanced version named Agile Wrist was later proposed by Angeles *et al.* in 2000 [15].

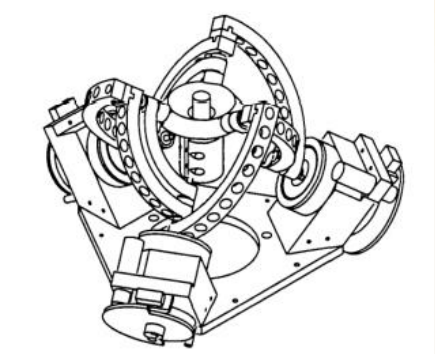

Fig. 10: Agile Eye SPM [13]

Fig. 11: Agile Wrist SPM [15]

[13] C. M. Gosselin and J.-F. Hamel, "The Agile Eye: a high-performance three-degree-of-freedom camera-orienting device," in Proceedings of the 1994 IEEE International Conference on Robotics and Automation (ICRA), pp. 781–786, 1994.

[14] X. Kong and C. M. Gosselin, "A formula that produces a unique solution to the forward displacement analysis of a quadratic spherical parallel manipulator: the Agile Eye," Journal of Mechanisms and Robotics, vol. 2, no. 4, 2009.

[15] J. Angeles, A. Morozov, L. Slutski, O. Navarro, and L. Jabre, "The modular design of a long-reach, 11-axis manipulator," in Romansy 13, pp. 225–233, Springer, 2000.

Introduction

Background Research and Literature Review

- Application-specific manipulator, SHaDe (Spherical Haptic Device), was developed in 2002 [16]. It was created to be used for the teleoperation as the master device of the Agile Eye.
- One more master haptic device based on the 3-RRR SPM was developed by Saafi *et al.* [17] in 2015. It is redundantly actuated to eliminate some of the manipulator's singularities.

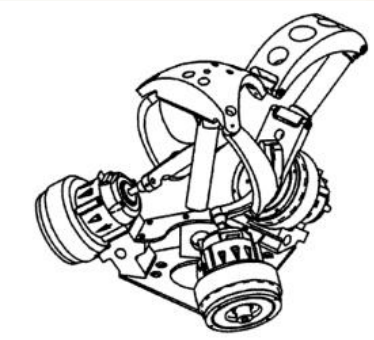

Fig. 12: SHaDe [16]

Fig. 13: Haptic device [17]

[16] L. Birglen, C. M. Gosselin, N. Pouliot, B. Monsarrat, and T. Laliberte, "SHaDe, a new 3-DOF haptic device," IEEE Transactions on Robotics and Automation, vol. 18, no. 2, pp. 166–175, 2002.
[17] H. Saafi, M. A. Laribi, and S. Zeghloul, "Optimal haptic control of a redundant 3-RRR spherical parallel manipulator," in 2015 IEEE/RSJ International Conference on Intelligent Robots and Systems (IROS), pp. 2591–2596, 2015.

Introduction

Background Research and Literature Review

Other SPMs with different architectures are:

- Argos by Vischer and Clavel (2000) [18] able to achieve ±60° in roll angle. It is a 3-DOF 3-R(2R/2S)S SPM.
- In 2000s, Rosheim and Sofka *et al.* [20] developed Omni-Wrist III (4-RRRR type) with 180° singularity-free semi-spherical movement. Variations like Omni-Wrist V (3-RSR-SS) and Omni-Wrist VI (4-RSR-SS) exist.
  ESPR RPM with 2 DOFs. Patented.

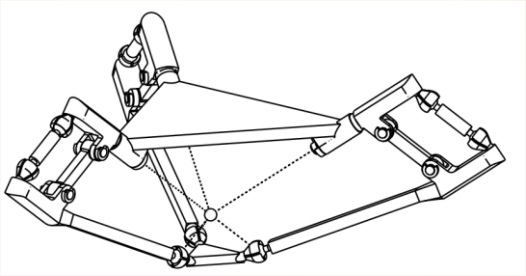

Fig. 14: Argos [19]

Fig. 15: Omni-Wrist III [20]

[18] P. Vischer and R. Clavel, “Kinematic calibration of the parallel Argos mechanism,” Robotica, vol. 18, no. 6, pp. 589–599, 2000.
[19] Gosselin, Clément M., and Jing Wang. "Singularity loci of a special class of spherical three-degree-of-freedom parallel mechanisms with revolute actuators." The International Journal of Robotics Research 21, no. 7 (2002): 649-659.
[20] M. E. Rosheim and G. F. Sauter, “New high-angulation omni-directional sensor mount,” in SPIE Free-Space Laser Communication and Laser Imaging II, pp. 163–174, 2002.

Introduction

Background Research and Literature Review

- The referenced works have limited roll-rotation of SPM's mobile platform around its normal vector.
- Coaxial SPM – a special case of the general SPM with a collinear (coaxial) arrangement of its input axes does not have this limitation.
- Coaxial SPM has extended full-circle (and unlimited) roll-rotation.
- First mentioned by Asada and Granito [5].

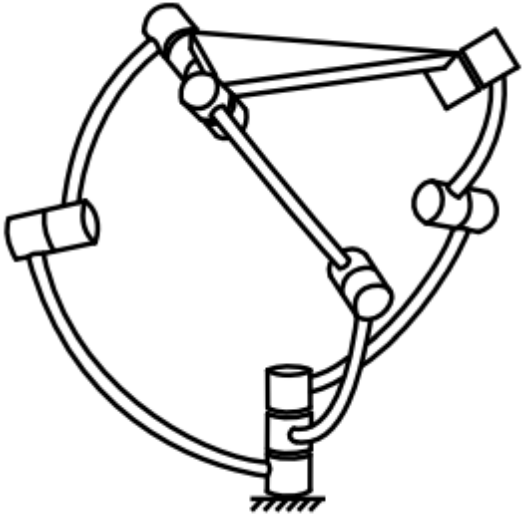

Fig. 16: Coaxial SPM

Introduction

Background Research and Literature Review

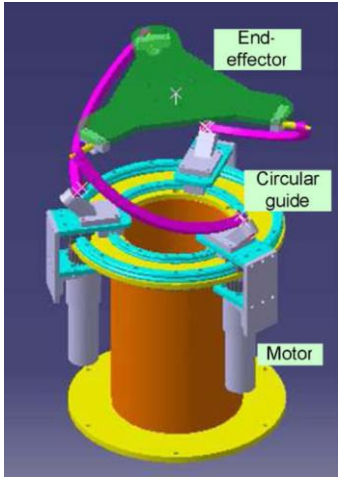

Fig. 17: Conceptual design of coaxial SPM by Bai (2009) [21]

Fig. 18: Coaxial SPM by Sudki *et al.* (2014) [22]

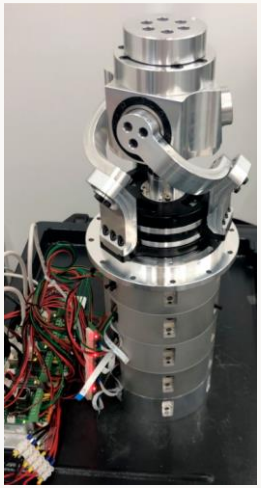

Fig. 19: CoSMo module by Noh *et al.* (2018) [23]

[21] S. Bai, "Optimum design of spherical parallel manipulators for a prescribed workspace," Mechanism and Machine Theory, vol. 45, no. 2, pp. 200–211, 2010.
[22] B. Sudki, M. Lauria, and F. Noca, "Robotic penguin-like propulsor with novel spherical joint," in Proceedings of the Third International Symposium on Marine Propulsors, 2013.
[23] J. Noh, J. Lee, W. Yang, and S. Lee, "Design of a concentrically stacked modular actuator with forced air cooling for multi-DOF robotic systems," Energies, vol. 11, no. 11, 2018.

Introduction

Background Research and Literature Review

- Asymmetrical SPMs and other not 3-RRR type SPMs were proposed as well.
- Their kinematic analysis is very complicated.
- Their design is tailored to a specific application.

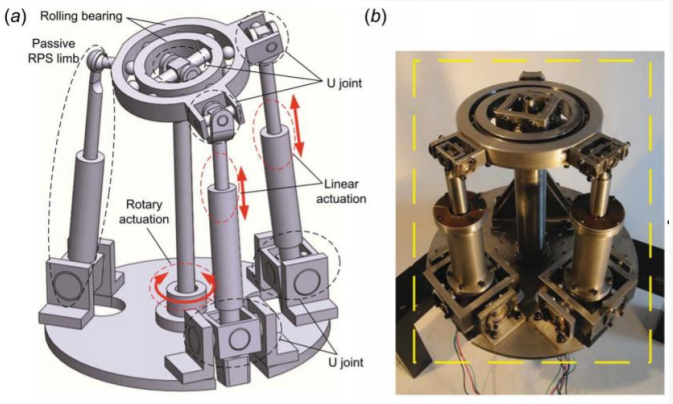

Fig. 20: 2UPU-RUR-RPS asymmetrical SPM [24]

[24] G. Wu, "Parameter-excited instabilities of a 2UPU-RUR-RPS spherical parallel manipulator with a driven universal joint," Journal of Mechanical Design, vol. 140, no. 9, 2018.

Introduction

Background Research and Literature Review

SPM Type	DOFs	Actuators	Unlimited Roll	Notes
Agile Eye/Agile Wrist [13, 15]	3	3	Limited to ±30°	Limited roll
Coaxial SPM by Bai [21]	3	3	Available	Issues with a circular guide, no demonstrated control
Coaxial SPM by Sudki [22]	3	3	Available	No demonstrated analysis, real-time control
CoSMo module [23]	3	4	Available	Little detail about infinite rotation. No target tracking and stabilization
Asymmetrical SPMs	2-3	3-4	Available or limited	Very complicated kinematic analysis
Coaxial SPM under study	3	3	Available	With kinematic analysis, control and application demonstration

Introduction

Background Research and Literature Review

Research Gap:

- No research has been published studying infinite rolling and its effects on manipulator's workspace and control strategies. No exploits of this distinct feature.
- Limited application examples showing only ability to move. Usage of the coaxial SPM as tracker and stabilization platform has never been done.

Novelty:

- Study of the effects of the infinite rolling on coaxial SPM's workspace and control strategies.
- Implemented real-time orientation, target tracking and stabilization control.

Kinematic Analysis

Kinematic Model

- Structure: *mobile platform* (1), *base*, *proximal* (3) and *distal* (2) *links.* γ = 0°.
- Joints defined by unit vectors $\mathbf{u}_i$, $\mathbf{w}_i$, and $\mathbf{v}_i$ for i = 1, 2, 3 from a *center of rotation.* Ref. frame shown in blue.
- Orientation of the coaxial SPM is described by unit vectors $\mathbf{v}_i$.
- Input joint positions defined as $\boldsymbol{\theta} \triangleq [\theta_1, \theta_2, \theta_3]^T$.

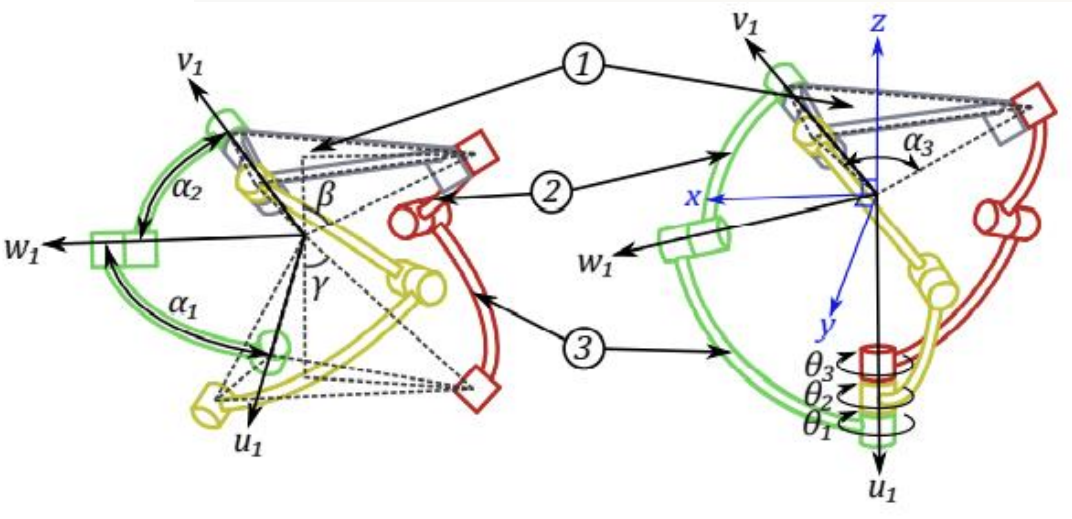

Fig. 21: Kinematic model of SPM

Kinematic Analysis

Kinematic Model

- Home configuration: $\boldsymbol{\theta} = [0, 0, 0]^T$.
- Rotation by angle σ preserving the direction of its normal vector **n** is achieved by calculating new instants of unit vectors $\mathbf{v}_{i,rot}$, $i = 1, 2, 3$, using the Rodrigues' rotation formula:

$$\mathbf{v}_{i,rot} = \mathbf{v}_i \cos\sigma + (\mathbf{v}_i \times \mathbf{n}) \sin\sigma + \mathbf{n}(\mathbf{n} \cdot \mathbf{v}_i)(1 - \cos\sigma), \quad i = 1, 2, 3 \qquad (1)$$

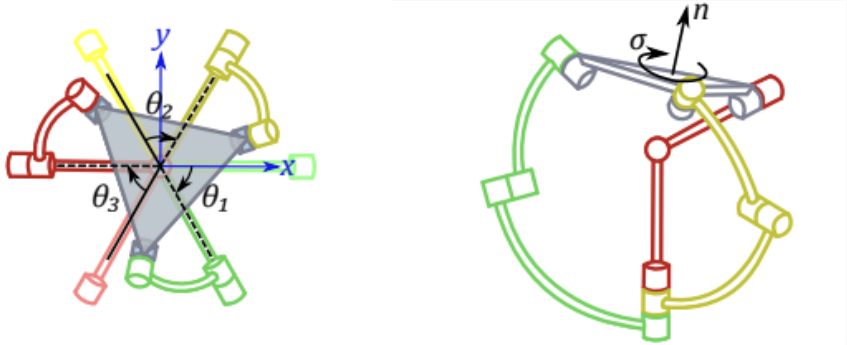

Fig. 22: Home configuration and roll-rotation

Kinematic Analysis

Forward Kinematics

Forward kinematic problem: given input joint variables, **θ**, to find each possible orientation (pose) of the mobile platform, i.e., the unit vectors $\mathbf{v}_i$, i = 1, 2, 3, resulting from it.

A system equations can be derived from geometric constraints:

$$\begin{cases} \mathbf{w}_i \cdot \mathbf{v}_i = \cos\alpha_2, \quad i = 1,2,3, \\ \mathbf{v}_i \cdot \mathbf{v}_j = \cos\alpha_3, \quad i,j = 1,2,3, \quad i \neq j, \\ \|\mathbf{v}_i\| = 1, \end{cases} \tag{2}$$

where $\alpha_3 = 2\sin^{-1}(\sin(\beta)\cdot\cos(\pi/6))$ is the angle between axes of the *i-th* and *j-th* mobile platform joints, and $\|\cdot\|$ is the Euclidean norm.

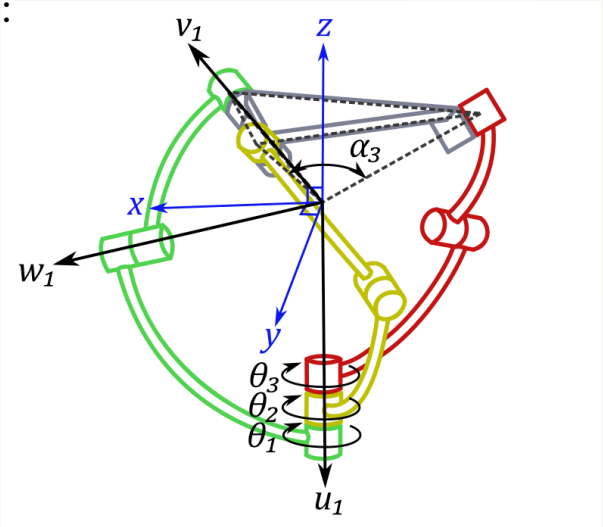

Fig. 23: Coaxial SPM model

Kinematic Analysis

Forward Kinematics

- This system is nonlinear and can not be solved in a closed form.
- An approach based on numerical method can be used instead.
- In this work, *trust-region* numerical optimization method was used implemented in MATLAB's *fsolve* function. It requires an initial guess vector:

$$\boldsymbol{x}_0 = \left[v_{1x}, v_{1y}, v_{1z}, v_{2x}, v_{2y}, v_{2z}, v_{3x}, v_{3y}, v_{3z} \right]^T \quad (3)$$

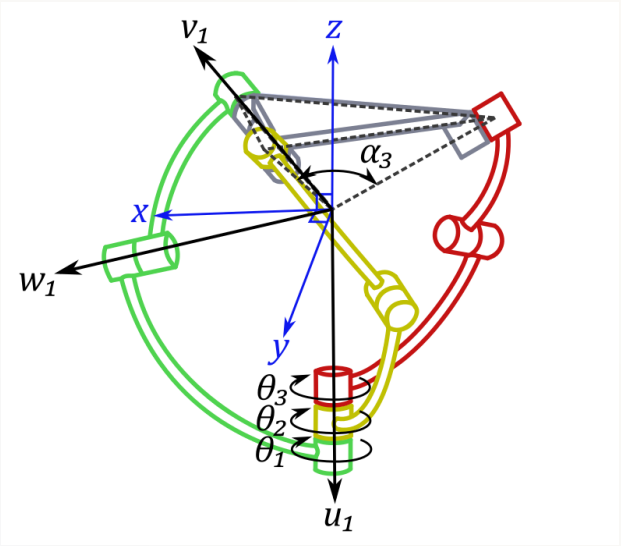

Fig. 23: Coaxial SPM model

Kinematic Analysis

Forward Kinematics

Algorithm 1: Obtaining a unique solution of the forward kinematic problem of a coaxial SPM

Input: $\boldsymbol{\theta}$, α_1, α_2, β, $\boldsymbol{x}_0$, η_i, $i = 1, 2, 3$
Output: Unique unit vectors $\mathbf{v}_i$, $i = 1, 2, 3$

Calculate $\alpha_3 = 2\sin^{-1}\left(\sin\beta\cos\frac{\pi}{6}\right)$;
for $i \leftarrow 1$ **to** 3 **do**
    Calculate $\mathbf{w}_i$ given $\boldsymbol{\theta}$;
    Calculate $\mathbf{w}_{i,rot}$ similar to (1);
Calculate initial guess vector $\boldsymbol{x}_0$ using (3) and $\mathbf{w}_{i,rot}$;
Calculate $\mathbf{v}_i$, $i = 1, 2, 3$, by solving system of equations (2) numerically, given $\mathbf{w}_i$, $i = 1, 2, 3$, with initial guess vector $\boldsymbol{x}_0$;

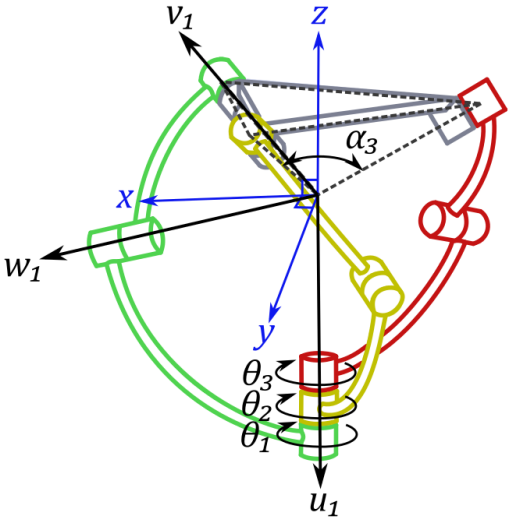

Fig. 23: Coaxial SPM model

Kinematic Analysis

Forward Kinematics Example 1

Input joint positions: $\boldsymbol{\theta} = [0, 0, 0]^T$, $\alpha_1 = 45°$, $\alpha_2 = 90°$, $\beta = 60° \rightarrow$ 8 solutions (assembly modes)

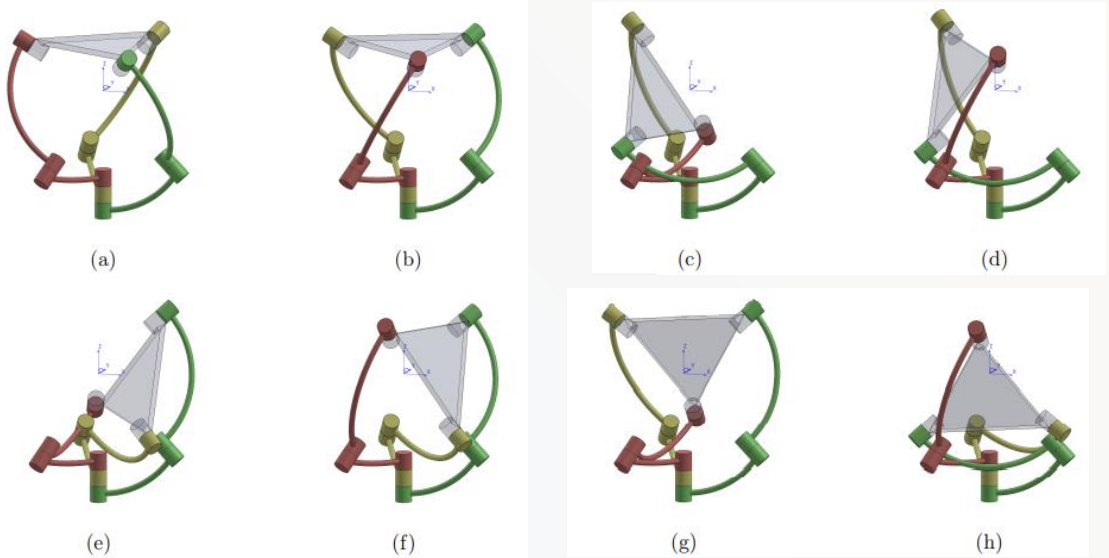

Fig. 24: Example 1 FK solutions

Kinematic Analysis

Forward Kinematics Example 2

Input joint positions: $\boldsymbol{\theta} = [60°, 90°, 120°]^T$, $\alpha_1 = 45°$, $\alpha_2 = 90°$, $\beta = 90° \rightarrow$ 8 solutions (assembly modes)

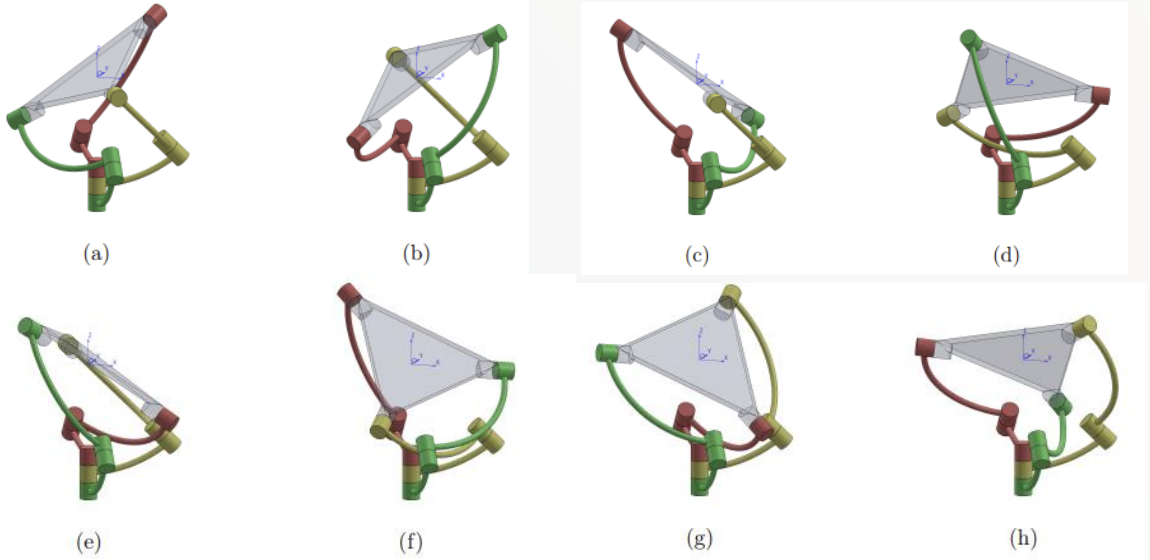

Fig. 25: Example 2 FK solutions

Kinematic Analysis

Forward Kinematics Examples

Orientation	$\mathbf{v}_1^T$	$\mathbf{v}_2^T$	$\mathbf{v}_3^T$
Fig. 24(a) CAD	$[0.500, -0.707, 0.500]$	$[0.362, 0.787, 0.500]$	$[-0.862, -0.079, 0.500]$
Fig. 24(a) calculated	$[0.5000, -0.7071, 0.5000]$	$[0.3624, 0.7866, 0.5000]$	$[-0.8624, -0.0795, 0.5000]$
Fig. 24(b) CAD	$[0.500, 0.707, 0.500]$	$[-0.862, 0.079, 0.500]$	$[0.362, -0.787, 0.500]$
Fig. 24(b) calculated	$[0.5000, 0.7071, 0.5000]$	$[-0.8624, 0.0795, 0.5000]$	$[0.3624, -0.7866, 0.5000]$
Fig. 25(a) CAD	$[-0.862, 0.079, -0.500]$	$[0.500, -0.866, 0.000]$	$[0.362, 0.787, 0.500]$
Fig. 25(a) calculated	$[-0.8625, 0.0791, -0.4998]$	$[0.5001, -0.8659, 0.0002]$	$[0.3620, 0.7866, 0.5002]$
Fig. 25(b) CAD	$[0.862, -0.079, 0.500]$	$[-0.500, 0.866, 0.000]$	$[-0.362, -0.787, -0.500]$
Fig. 25(b) calculated	$[0.8622, -0.0798, 0.5002]$	$[-0.4999, 0.8661, 0.0002]$	$[-0.3627, -0.7865, -0.4998]$

Kinematic Analysis

Inverse Kinematics

Inverse kinematic problem: given orientation (pose) of the mobile platform, i.e., the unit vectors $\mathbf{v}_i$, i = 1, 2, 3, to find each possible input joint variables, $\boldsymbol{\theta}$, resulting in it.

Three uncoupled equations used to compute each of input joint variable θ_i, i = 1, 2, 3, are formulated as [25]:

$$A_i T_i^2 + 2 B_i T_i + C_i = 0, \quad i = 1, 2, 3, \tag{4}$$

with

$$T_i = \tan\left(\frac{\theta_i}{2}\right). \tag{5}$$

$$\begin{aligned} A_i &= -\cos\eta_i \sin\alpha_1 v_{ix} - \sin\eta_i \sin\alpha_1 v_{iy} - \cos\alpha_1 v_{iz} - \cos\alpha_2; \\ B_i &= \sin\eta_i \sin\alpha_1 v_{ix} - \cos\eta_i \sin\alpha_1 v_{iy}; \\ C_i &= \cos\eta_i \sin\alpha_1 v_{ix} + \sin\eta_i \sin\alpha_1 v_{iy} - \cos\alpha_1 v_{iz} - \cos\alpha_2, \end{aligned} \tag{6}$$

where v_{ix}, v_{iy}, and v_{iz} are components of the unit vectors $\mathbf{v}_i$, i = 1, 2, 3.

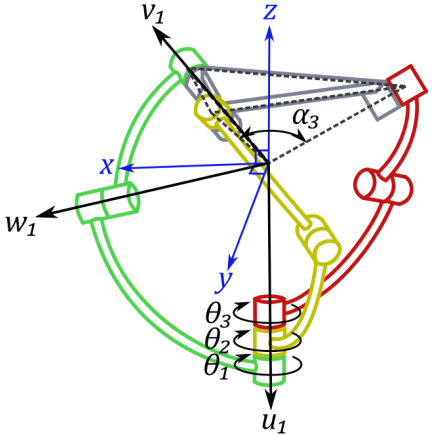

Fig. 23: Coaxial SPM model

[25] C. M. Gosselin and E. Lavoie, "On the kinematic design of spherical three-degree-of-freedom parallel manipulators," The International Journal of Robotics Research, vol. 12, no. 4, pp. 394–402, 1993.

Kinematic Analysis

Inverse Kinematics

Algorithm 2: Obtaining a unique solution of the inverse kinematics problem of a coaxial SPM

Input: $\mathbf{v}_i$, $i = 1, 2, 3$, α_1, α_2, η_i
Output: Input joint positions vector $\boldsymbol{\theta}$

for $i \leftarrow 1$ **to** 3 **do**
  Calculate A_i, B_i, C_i using (6) given $\mathbf{v}_i$;
  Solve equation (5) for T_i;
  Find θ_i using equation (4) and select a solution coming from the root with added or subtracted square root of the discriminant for *l-l-l* or *r-r-r* working mode, respectively;
return θ_i, $i = 1, 2, 3$

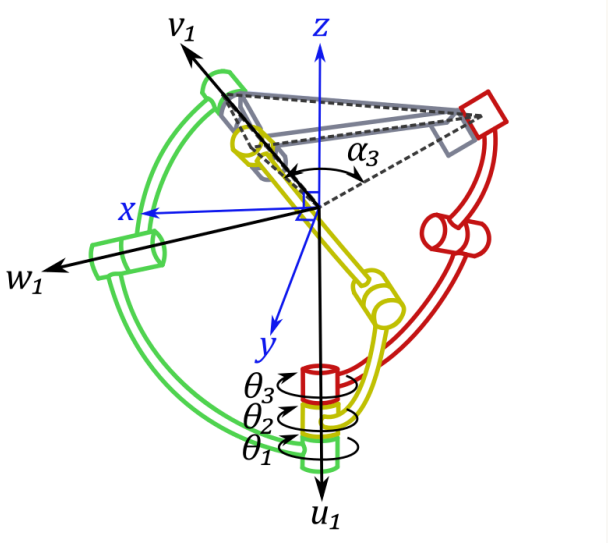

Fig. 23: Coaxial SPM model

Kinematic Analysis

Inverse Kinematics Example 1

Pose taken from Fig. 24a, $\alpha_1 = 45°$, $\alpha_2 = 90°$, $\beta = 60° \rightarrow$ 8 solutions (working modes)

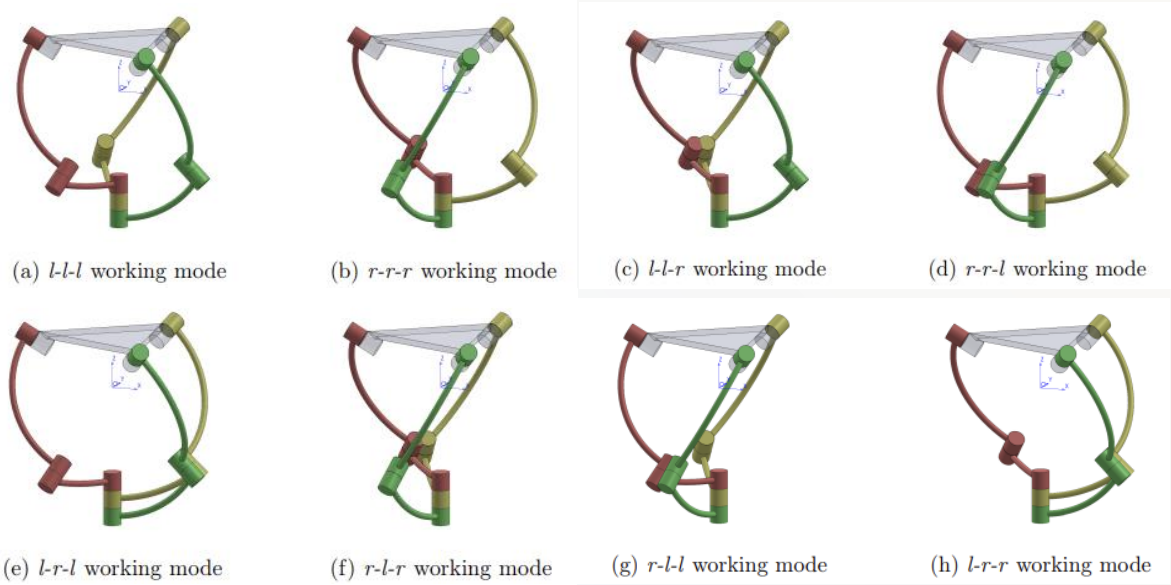

Fig. 26: Example 2 IK solutions

Kinematic Analysis

Inverse Kinematics Example 2

Pose taken from Fig. 25a, α_1 = 45°, α_2 = 90°, β = 60° → 8 solutions (working modes)

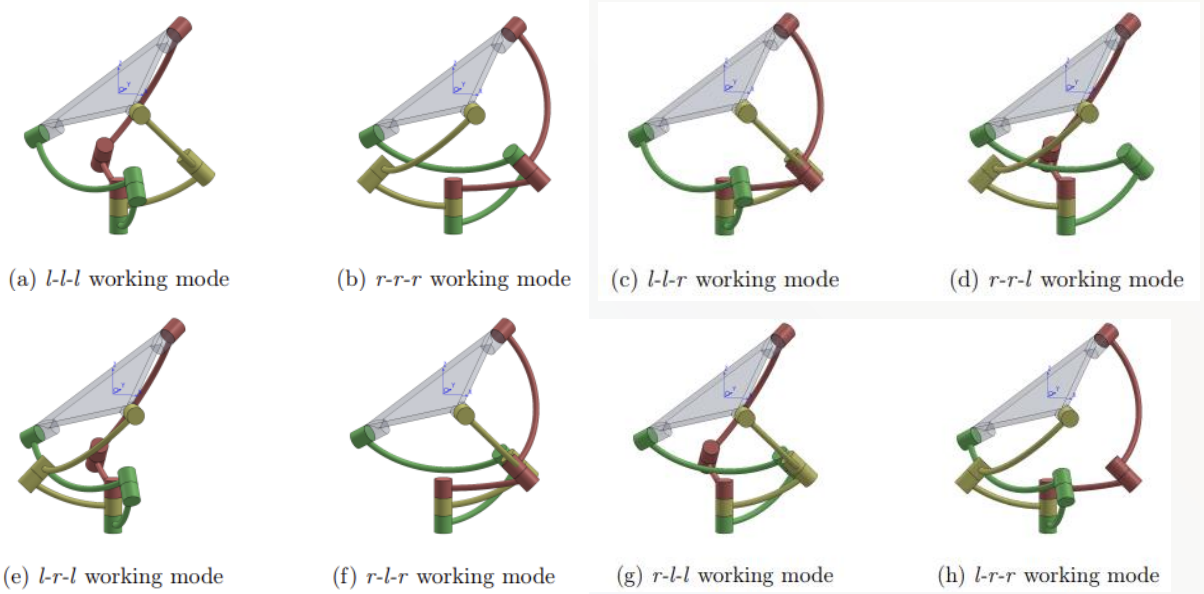

Fig. 27: Example 2 IK solutions

Kinematic Analysis

Inverse Kinematics Examples

Orientation	$\mathbf{v}$	$\boldsymbol{\theta}_{CAD}$	$\boldsymbol{\theta}_{calculated}$
Fig. 26(a)	$\begin{bmatrix} 0.500 & 0.362 & -0.862 \\ -0.707 & 0.787 & -0.079 \\ 0.500 & 0.500 & 0.500 \end{bmatrix}$	$\begin{bmatrix} 0.00° \\ 0.00° \\ 0.00° \end{bmatrix}$	$\begin{bmatrix} 0.0000° \\ -0.0455° \\ 0.0473° \end{bmatrix}$
Fig. 26(b)	$\begin{bmatrix} 0.500 & 0.362 & -0.862 \\ -0.707 & 0.787 & -0.079 \\ 0.500 & 0.500 & 0.500 \end{bmatrix}$	$\begin{bmatrix} 109.47° \\ 109.47° \\ 109.47° \end{bmatrix}$	$\begin{bmatrix} 109.4631° \\ 109.4480° \\ 109.4799° \end{bmatrix}$
Fig. 27(a)	$\begin{bmatrix} -0.862 & 0.500 & 0.362 \\ 0.079 & -0.866 & 0.787 \\ -0.500 & 0.000 & 0.500 \end{bmatrix}$	$\begin{bmatrix} 60.00° \\ 90.00° \\ 120.00° \end{bmatrix}$	$\begin{bmatrix} 59.9527° \\ 89.9993° \\ 119.9545° \end{bmatrix}$
Fig. 27(b)	$\begin{bmatrix} -0.862 & 0.500 & 0.362 \\ 0.079 & -0.866 & 0.787 \\ -0.500 & 0.000 & 0.500 \end{bmatrix}$	$\begin{bmatrix} 310.53° \\ 270.00° \\ 229.47° \end{bmatrix}$	$\begin{bmatrix} -49.4799° \\ -90.0007° \\ -130.5520° \end{bmatrix}$

Kinematic Analysis

Conference Publication

Results were presented at IEEE CASE 2019, Vancouver, Canada:

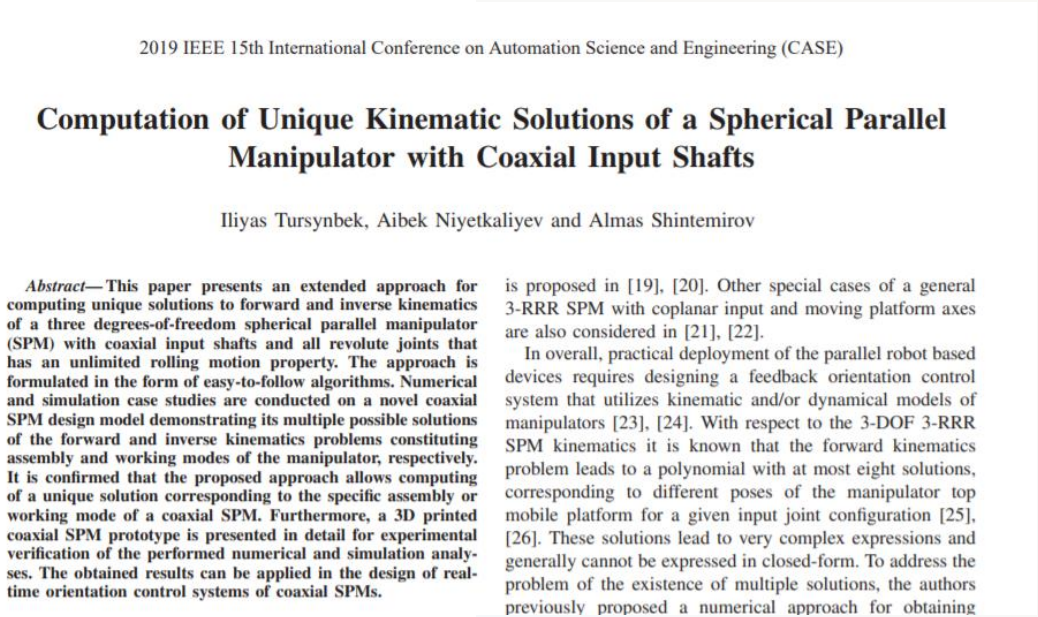

2019 IEEE 15th International Conference on Automation Science and Engineering (CASE)

Computation of Unique Kinematic Solutions of a Spherical Parallel Manipulator with Coaxial Input Shafts

Iliyas Tursynbek, Aibek Niyetkaliyev and Almas Shintemirov

***Abstract*— This paper presents an extended approach for computing unique solutions to forward and inverse kinematics of a three degrees-of-freedom spherical parallel manipulator (SPM) with coaxial input shafts and all revolute joints that has an unlimited rolling motion property. The approach is formulated in the form of easy-to-follow algorithms. Numerical and simulation case studies are conducted on a novel coaxial SPM design model demonstrating its multiple possible solutions of the forward and inverse kinematics problems constituting assembly and working modes of the manipulator, respectively. It is confirmed that the proposed approach allows computing of a unique solution corresponding to the specific assembly or working mode of a coaxial SPM. Furthermore, a 3D printed coaxial SPM prototype is presented in detail for experimental verification of the performed numerical and simulation analyses. The obtained results can be applied in the design of real-time orientation control systems of coaxial SPMs.**

is proposed in [19], [20]. Other special cases of a general 3-RRR SPM with coplanar input and moving platform axes are also considered in [21], [22].

In overall, practical deployment of the parallel robot based devices requires designing a feedback orientation control system that utilizes kinematic and/or dynamical models of manipulators [23], [24]. With respect to the 3-DOF 3-RRR SPM kinematics it is known that the forward kinematics problem leads to a polynomial with at most eight solutions, corresponding to different poses of the manipulator top mobile platform for a given input joint configuration [25], [26]. These solutions lead to very complex expressions and generally cannot be expressed in closed-form. To address the problem of the existence of multiple solutions, the authors previously proposed a numerical approach for obtaining

NAZARBAYEV UNIVERSITY

Kinematic Analysis

Infinite Rotational Motion

Rotation around vector **n** computed as:

$$\begin{cases} \mathbf{n} = \dfrac{\mathbf{v}_1 + \mathbf{v}_2 + \mathbf{v}_3}{\|\mathbf{v}_1 + \mathbf{v}_2 + \mathbf{v}_3\|}, & \forall \beta \neq 90°, \\ \mathbf{n} = \dfrac{\mathbf{v}_1 \times \mathbf{v}_2}{\|\mathbf{v}_1 \times \mathbf{v}_2\|}, & \forall \beta = 90°. \end{cases} \quad (7)$$

The rotational motion is sampled into a sequence of S instants with the rotation angles as (assume uniform sampling):

$$\boldsymbol{\sigma} = \{\sigma_1,\ \sigma_2,\ \ldots\ \sigma_S\}.$$

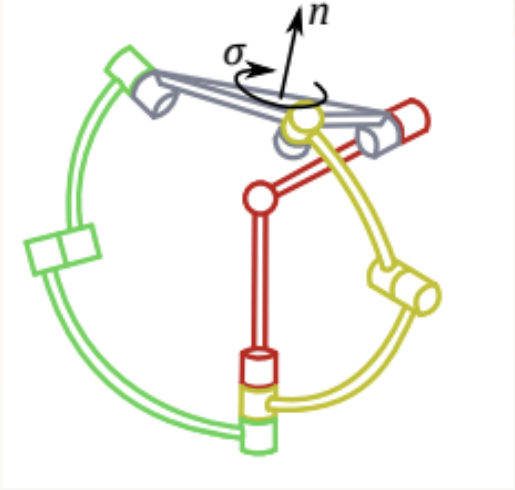

Fig. 28: Roll-rotation

At each sampling instant, calculated with the Rodrigues' rotation formula, a unique inverse kinematic solution is obtained. Algorithm 2 returns results in the closed interval −180° (−π) to +180° (+π). It has to be accounted for and adjusted.

Kinematic Analysis

Infinite Rotational Motion

Algorithm 3: Generation of an input joints trajectory for a full-circle rotational motion of a coaxial SPM

Input: $\mathbf{v}_i$, $i = 1, 2, 3$, α_1, α_2, η_i, $\boldsymbol{\sigma}$
Output: Input joints trajectory $\boldsymbol{\theta}_{traj}$

Calculate $\mathbf{n}$ using (7) given $\mathbf{v}_i$;
for $j \leftarrow 1$ **to** S **do**
  Calculate $\mathbf{v}_{i,j}$, $i = 1, 2, 3$, using (1) with σ_j and $\mathbf{n}$;
  Calculate input joint positions $\boldsymbol{\theta}_j$ for each $\mathbf{v}_{i,j}$, $i = 1, 2, 3$, using Algorithm 2;
  $\boldsymbol{\theta}_{traj}(j) \leftarrow \boldsymbol{\theta}_j$;

/* check for 360° jumps in $\boldsymbol{\theta}_{traj}$ */
for $k \leftarrow 1$ **to** $S - 1$ **do**
  if $\theta_{1,k} - \theta_{1,k+1} > 0°$ **then**
    $\theta_{1,k+1} = \theta_{1,k+1} + 360°$;
  if $\theta_{2,k} - \theta_{2,k+1} > 0°$ **then**
    $\theta_{2,k+1} = \theta_{2,k+1} + 360°$;
  if $\theta_{3,k} - \theta_{3,k+1} > 0°$ **then**
    $\theta_{3,k+1} = \theta_{3,k+1} + 360°$;

/* check for link surpass */
if $\theta_{3,1} - \theta_{2,1} > 120°$ **then**
  $\theta_{2,1\ldots S} = \theta_{2,1\ldots S} + 360°$;
if $\theta_{2,1} - \theta_{1,1} > 120°$ **then**
  $\theta_{1,1\ldots S} = \theta_{1,1\ldots S} + 360°$;
if $\theta_{1,1} - \theta_{3,1} > 120°$ **then**
  $\theta_{3,1\ldots S} = \theta_{3,1\ldots S} + 360°$;
return $\boldsymbol{\theta}_{traj}$

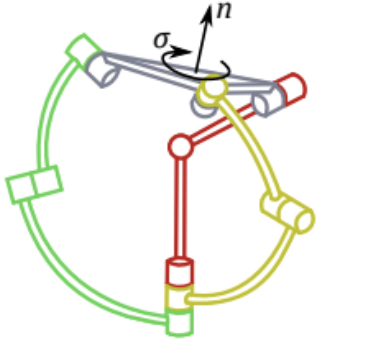

Fig. 28: Roll-rotation

Kinematic Analysis

Conference Publication

Results were presented at IEEE/ASME AIM 2020, Boston, USA (virtual mode):

2020 IEEE/ASME International Conference on
Advanced Intelligent Mechatronics (AIM), Boston, USA
(Virtual Conference), July 6-9, 2020

Infinite Torsional Motion Generation of a Spherical Parallel Manipulator with Coaxial Input Axes

Iliyas Tursynbek and Almas Shintemirov

***Abstract*— One of the distinct features of 3-RRR spherical parallel manipulators with coaxial input axes (coaxial SPM) is the ability to perform infinite torsional motion of the manipulator mobile platform around its normal vectors. This paper presents a novel approach for infinite torsional motion generation of the coaxial SPM based on the author's revised approach for obtaining unique solutions to SPM kinematics and the methodology for numerical computation of the SPM configuration workspace. Numerical results demonstrate the application of the proposed approach for computing infinite torsional motion of a 3D model of a novel coaxial SPM design.**

the previously developed approach for computing unique forward and inverse kinematics solutions of a general 3-DOF 3-RRR SPM [21], which was also utilized in the development of offline motion planning and real-time orientation control frameworks for general SPMs in [22], [23].

The paper is organized as follows. Section II gives an overview of the coaxial SPM kinematics, whereas the generation of infinite torsional motions is presented in Section III. Subsequently, Section IV outlines the effects of singularities and link collisions on the coaxial SPM configuration space

Experimental Setup

Simulation Model and Mechanical Prototype

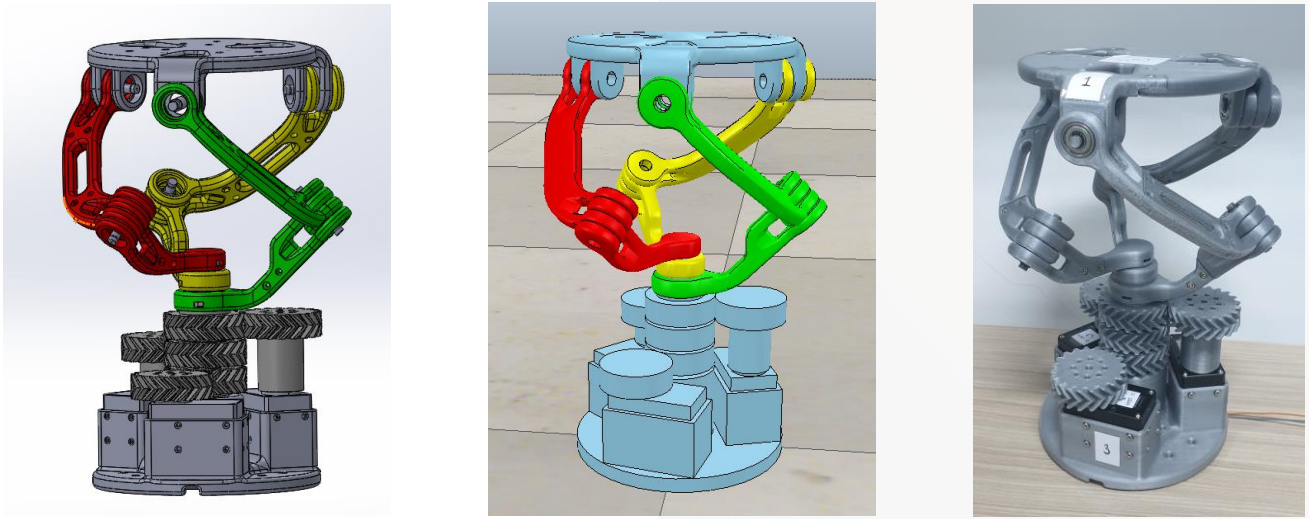

Fig. 29: Coaxial SPM: CAD model (left), simulation model (middle), mechanical prototype (right)

Experimental Setup

Simulation Model and Mechanical Prototype

$\alpha_1 = 45°, \alpha_2 = 90°, \beta = 90°$

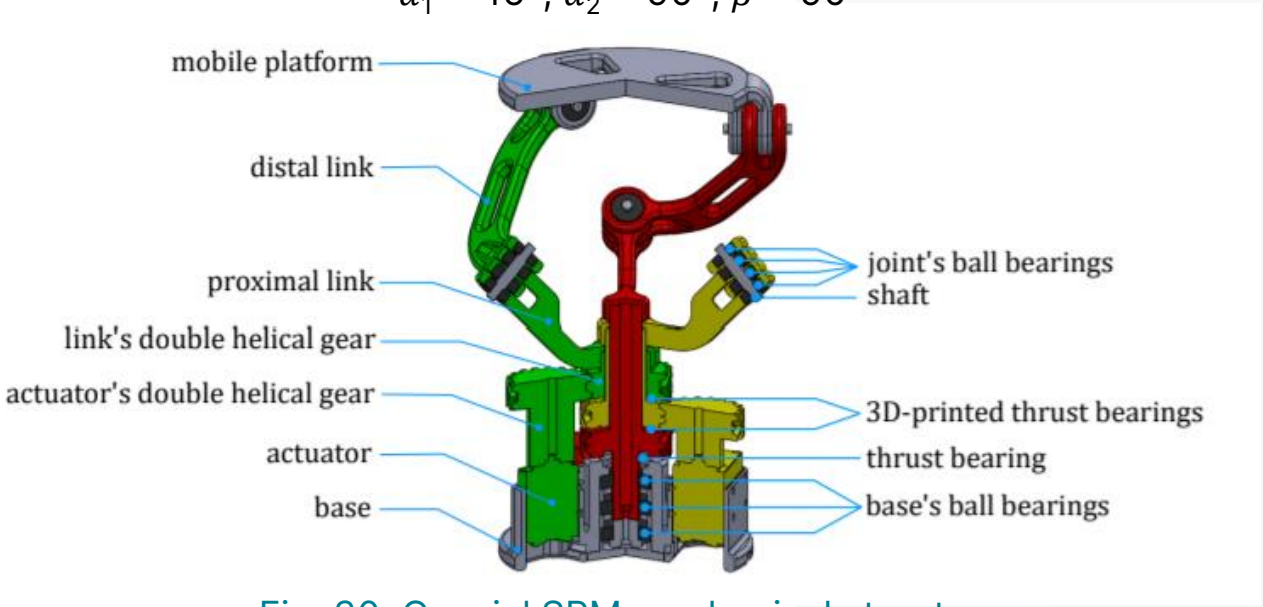

Fig. 30: Coaxial SPM mechanical structure

Experimental Setup

Simulation Model and Mechanical Prototype

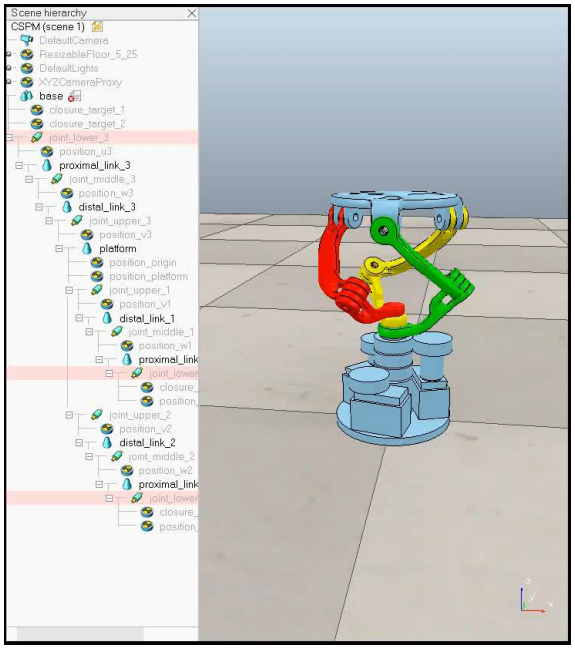

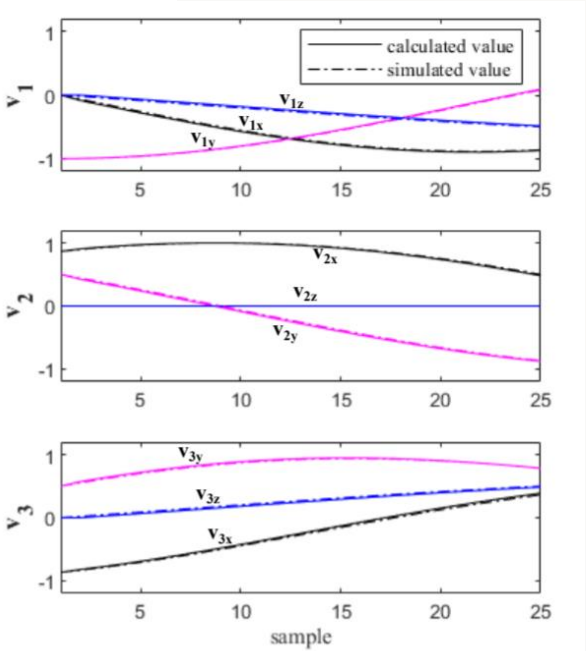

Fig. 31: Calculated vs. simulated orientation

MATLAB®

position ⇕ pose + collision

CoppeliaSim
from the creators of V-REP

NAZARBAYEV UNIVERSITY

Experimental Setup

Simulation Model and Mechanical Prototype

Results were presented at 2020 NIR (Nonlinearity, Information and Robotics) Conference, Russia (virtual mode):

Modeling and Simulation of Spherical Parallel Manipulators in CoppeliaSim (V-REP) Robot Simulator Software

Iliyas Tursynbek
Department of Robotics and Mechatronics
Nazarbayev University
Nur-Sultan, Kazakhstan
iliyas.tursynbek@nu.edu.kz

Almas Shintemirov
Department of Robotics and Mechatronics
Nazarbayev University
Nur-Sultan, Kazakhstan
ashintemirov@nu.edu.kz

***Abstract*—This paper presents a new methodology for modeling and simulation of spherical parallel manipulators (SPM) in CoppeliaSim (V-REP) robot simulator software. Using a SPM with coaxial input shafts as the case study, the steps for the robot SolidWorks CAD model importing, modeling in CoppeliaSim and interfacing with MATLAB for external control of the robot model are described in detail. The SPM motion simulation results are then presented and verified on an experimental 3D-printed system prototype.**

***Index Terms*—spherical parallel manipulator, robot simulation, collision detection, CoppeliaSim, V-REP**

prototypes. There is a plethora of simulation tools that allow to visualize and analyze kinematics and/or dynamics of PMs. Most of them are special simulators created for a particular problem or robot [5]–[10]. Among the general-purpose simulators, the most known example is *Gazebo* [11] developed by Open Source Robotics Foundation and used in DARPA Robotics Challenge [12]. Versions for Linux, macOS, Windows are available. It is also ROS [13] compatible. It supports the ODE, Bullet, Simbody and DART physics engines and can provide realistic 3D rendering. Custom plugins

NAZARBAYEV UNIVERSITY

Motion Planning

Link Collision Detection

- Link collision check routine is based on the simulations with the virtual model in CoppeliaSim.
- It has built-in link collision detection module based on the algorithm for efficient and exact interference detection among complex polygonal models (OBBTrees) [26].
- Collision check routine is repeated at each sampling instant and motion data can be saved for the following analysis, for example in MATLAB.

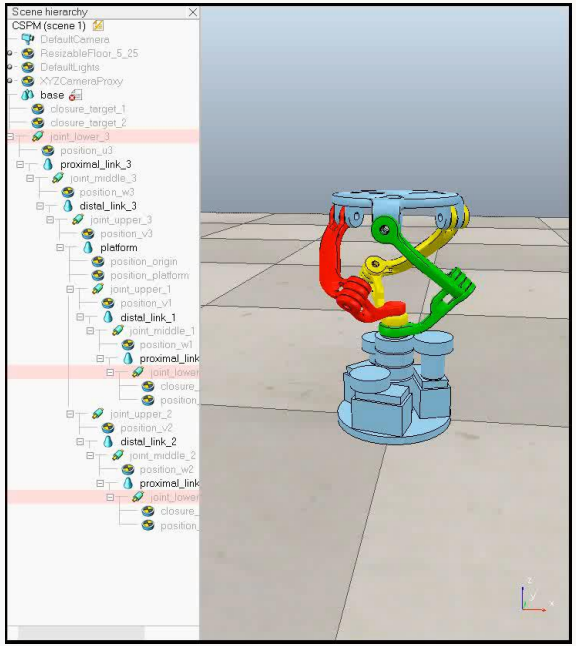

[26] S. Gottschalk, M. C. Lin, and D. Manocha, “OBBTree: A Hierarchical Structure for Rapid Interference Detection,” in Proceedings of the 23rd annual conference on Computer graphics and interactive techniques – ACM SIGGRAPH, pp. 171–180, 1996.

Motion Planning

Singularity Detection

- A singular configuration of a manipulator is a pose at which it gains or loses some of its DOFs.
- PMs have 3 types of singularities [27]:
    1. Type I – one the boundary of the workspace, when links are fully folded or unfolded
    2. Type II –within the workspace, usually not reachable because of the link interference
    3. Type I + Type II – happens only with specific link parameters
- For control purposes, it is necessary to keep a manipulator away from singular and near-singular configurations as its controllability is weak at these locations.

[27] C. M. Gosselin and J. Angeles, “Singularity analysis of closed-loop kinematic chains,” IEEE Transactions on Robotics and Automation, vol. 6, no. 3, pp. 281–290, 1990.

Motion Planning

Singularity Detection

Singularity analysis is based on the analysis of the relationship between the input joint rates and output angular velocity of the mobile platform as follows [27]:

$$\dot{\theta} = \mathbf{J}\omega, \tag{8}$$

where ω is the angular velocity of the mobile platform, $\dot{\theta}$ is the input joint rates, and **J** is the Jacobian matrix that maps the angular velocity ω to the input joint rates $\dot{\theta}$.

The Jacobian matrix can be defined as [27]:

$$\mathbf{J} = -\mathbf{J}_2^{-1}\mathbf{J}_1, \tag{9}$$

which leads to the equivalent representation of (8) written as:

$$\mathbf{J}_1\omega + \mathbf{J}_2\dot{\theta} = \mathbf{0} \tag{10}$$

Motion Planning

Singularity Detection

$\mathbf{J}_1$ and $\mathbf{J}_2$ are both n × n Jacobian matrices (n = 3 for coaxial SPM), and configuration dependent, i.e., $\mathbf{J}_1 = \mathbf{J}_1(\mathbf{v}_i, \theta)$ and $\mathbf{J}_2 = \mathbf{J}_2(\mathbf{v}_i, \theta)$.

For the 3-RRR type SPMs, these matrices are expressed as [27]:

$$\mathbf{J}_1 = \begin{bmatrix} (\mathbf{w}_1 \times \mathbf{v}_1)^T \\ (\mathbf{w}_2 \times \mathbf{v}_2)^T \\ (\mathbf{w}_3 \times \mathbf{v}_3)^T \end{bmatrix} \tag{11}$$

$$\mathbf{J}_2 = diag(\mathbf{w}_1 \times \mathbf{u}_1 \cdot \mathbf{v}_1, \mathbf{w}_2 \times \mathbf{u}_2 \cdot \mathbf{v}_2, \mathbf{w}_3 \times \mathbf{u}_3 \cdot \mathbf{v}_3). \tag{12}$$

Motion Planning

Singularity Detection

Conditioning index $\zeta(\mathbf{J}) \in (0, 1)$ is used to estimate the proximity of a particular SPM configuration to singularity [24]:

$$\zeta(\mathbf{J}) = \frac{1}{\|\mathbf{J}\| \, \|\mathbf{J}^{-1}\|}, \tag{13}$$

where $\|\mathbf{J}\|$ is estimated as:

$$\|\mathbf{J}\| = \sqrt{tr\left(\mathbf{J}^T \frac{1}{3}\mathbf{I}\mathbf{J}\right)}, \tag{14}$$

and $\mathbf{I}$ denotes a 3 × 3 identity matrix.

- $\zeta(\mathbf{J}) > \zeta(\mathbf{J})_{min}$ can be used as threshold parameter.
- $\zeta(\mathbf{J}) = 0$ input configurations is singular, $\zeta(\mathbf{J}) = 1$ input configurations is singular.

Motion Planning

Configuration Space

- One of the key concepts in motion planning is the configuration space (C-space) which is a set of all attainable input joint position, i.e., configurations.
- It provides information about which input commands are feasible and which are not.
- Smooth and (or) optimal input reference trajectories can be computed and verified using C-space.
- Feasible input joint positions are the one which are non-singular/near-singular and without link collisions. Singularity is calculated using the approach previously mentioned. Link collision checks are done with CoppeliaSim.

Motion Planning

Configuration Space

A 3D space of possible configurations is sample into 3D grid of test nodes.

Each node is tested for singularity. The ones with $\zeta(\mathbf{J}) > \zeta(\mathbf{J})_{\text{min}}$ are checked for link collision.

Algorithm 4: Numerical computation of the configuration space

Input: α_1, α_2, β, $\boldsymbol{x}_0$, η_i, ϕ_i, $i = 1, 2, 3$
Output: Set $\mathcal{V}$

$\mathcal{V} \leftarrow \emptyset$;
for $a_1 \leftarrow 1$ **to** N_1 **do**
  for $a_2 \leftarrow 1$ **to** N_2 **do**
    for $a_3 \leftarrow 1$ **to** N_3 **do**
      $singularity \leftarrow false$;
      $collision \leftarrow false$;
      /* link surpass check */
      if $\theta_3(a_3) - \theta_2(a_2) > 120°$ **or** $\theta_2(a_2) - \theta_1(a_1) > 120°$ **or** $\theta_1(a_1) - \theta_3(a_3) > 120°$ **then**
        $collision \leftarrow true$
        break
      $\boldsymbol{\theta} \leftarrow \left[\theta_1(a_1) \quad \theta_2(a_2) \quad \theta_3(a_3)\right]^T$;
      /* forward kinematics */
      Calculate $\mathbf{w}_i$ and $\mathbf{v}_i$, $i = 1, 2, 3$, given $\boldsymbol{\theta}$ using Algorithm 1;
      /* singularity detection */
      Calculate $\mathbf{J}$ given $\mathbf{u}_i$, $\mathbf{w}_i$ and $\mathbf{v}_i$, $i = 1, 2, 3$, following (4.2)-(4.5);
      Calculate $\zeta(\mathbf{J})$ given $\mathbf{J}$, following (4.6) and (4.7);
      if $\zeta(\boldsymbol{J}) < \zeta(\boldsymbol{J})_{min}$ **then**
        $singularity \leftarrow true$
        break
      /* link collision detection */
      Send $\boldsymbol{\theta}$ to the coaxial SPM motion simulator;
      if *collision handle* == 1 **then**
        $collision \leftarrow true$
        break
      /* update the space */
      if $singularity == false$ **and** $collision == false$ **then**
        $\mathcal{V} \leftarrow \mathcal{V} \cup \{\boldsymbol{\theta}\}$
return $\mathcal{V}$

Motion Planning

Configuration Space - Results

In total, a grid of 373,248 nodes was tested. A uniform sampling interval of δ_φ = 5° was used, resulting in 72 instants for each input joint position θ_i, i = 1, 2, 3. (72x72x72 = 373,248). $\zeta(\mathbf{J})_{\text{min}}$ = 0.2

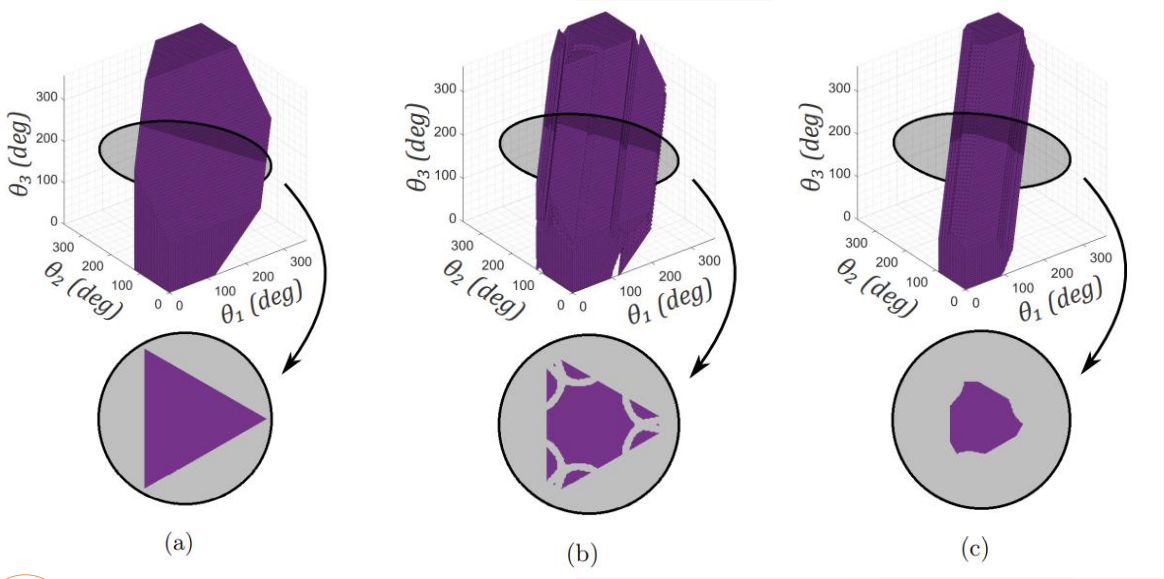

*unbounded C-space

Fig. 32: Steps in estimation of the feasible C-space

Motion Planning

Cartesian Workspace

Following a similar space sampling approach, the Cartesian workspace of the coaxial SPM is numerically computed. At each testing point, a rotational motion is checked and verified using simulation in CoppeliaSim for possible link collision during full-circle rotation.

- An icosahedral grid was used as the sampling basis
- Factor = 32
- 10,242 vertices, i.e., test points
- d_{min} = 0.0346 unit distance
- Rotation sampling with $\Delta(\psi) = 1^{\circ}$

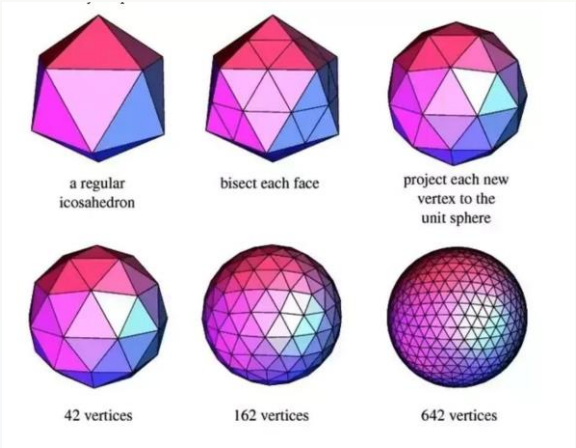

Fig. 33: Icosahedral grid

Motion Planning

Cartesian Workspace

Algorithm 5: Numerical computation of the Cartesian workspace

Input: l, $\boldsymbol{\sigma}$, α_1, α_2, β, $\boldsymbol{x}_0$, η_i, $i = 1, 2, 3$
Output: Set $\mathcal{W}$

$\mathcal{W} \leftarrow \emptyset$;
$\mathcal{W}_{temp} \leftarrow$ icosahedral grid generated using [320];
for $j \leftarrow 1$ **to** N **do**
  $singularity \leftarrow false$;
  $collision \leftarrow false$;
  Set test node coordinates as $\mathbf{n} = \mathcal{W}_{temp}(j)$;
  Reconstruct $\mathbf{v}_{i,j}$, $i = 1, 2, 3$, following (4.9)-(4.11);
  Generate rotational motion trajectory $\boldsymbol{\theta}_{traj}$ for a single rotation given $\mathbf{v}_{i,j}$, $i = 1, 2, 3$, using Algorithm 3;
  /* singularity detection */
  for $k \leftarrow 1$ **to** S **do**
    Calculate $\mathbf{w}_{i,j,k}$ and $\mathbf{v}_{i,j,k}$, $i = 1, 2, 3$, given $\boldsymbol{\theta}_{traj}(k)$ using Algorithm 1;
    Calculate $\mathbf{J}$ given $\mathbf{u}_{i,j,k}$, $\mathbf{w}_{i,j,k}$ and $\mathbf{v}_{i,j,k}$, $i = 1, 2, 3$, following (4.2)-(4.5);
    Calculate $\zeta(\mathbf{J})$ given $\mathbf{J}$, following (4.6) and (4.7);
    if $\zeta(\boldsymbol{J}) < \zeta(\boldsymbol{J})_{min}$ **then**
      $singularity \leftarrow true$
      break
  if $singularity == true$ **then**
    break
  /* link collision detection */
  Send $\boldsymbol{\theta}_{traj}$ to robot simulator;
  if *collision handle* $== 1$ **then**
    $collision \leftarrow true$
    break
  /* update the workspace */
  if $singularity == false$ **and** $collision == false$ **then**
    $\mathcal{W} \leftarrow \mathcal{W} \cup \mathbf{n}$
return $\mathcal{W}$

Motion Planning

Cartesian Workspace - Results

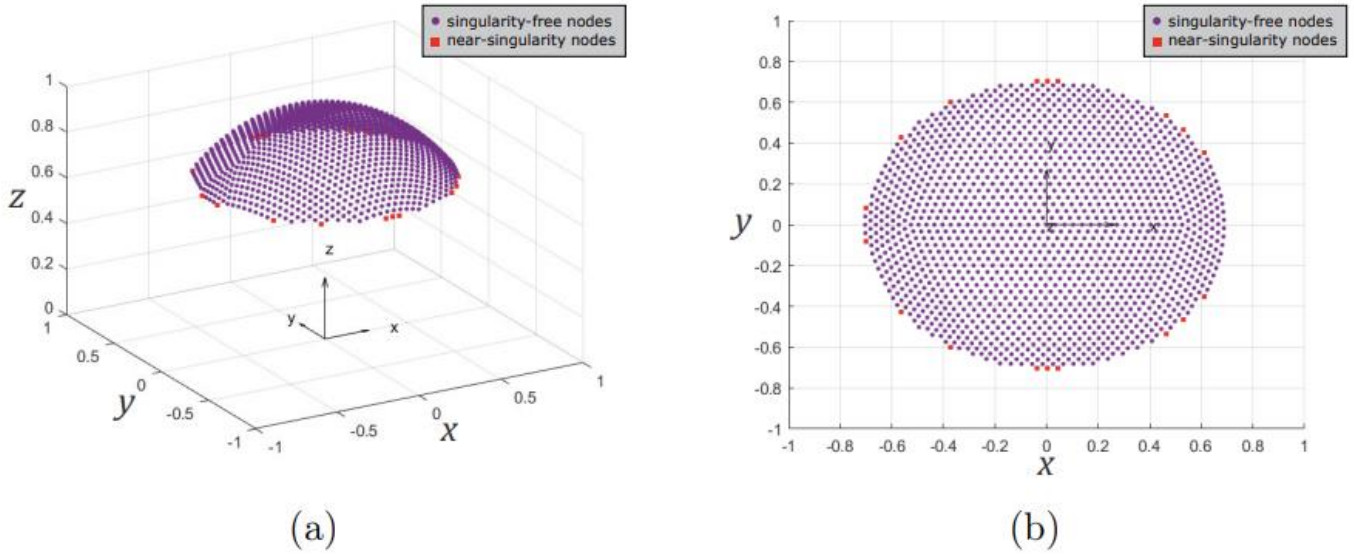

Fig. 34: Test points with detected near-singular poses ($\zeta(\mathbf{J})_{min} = 0.2$)

Motion Planning

Cartesian Workspace - Results

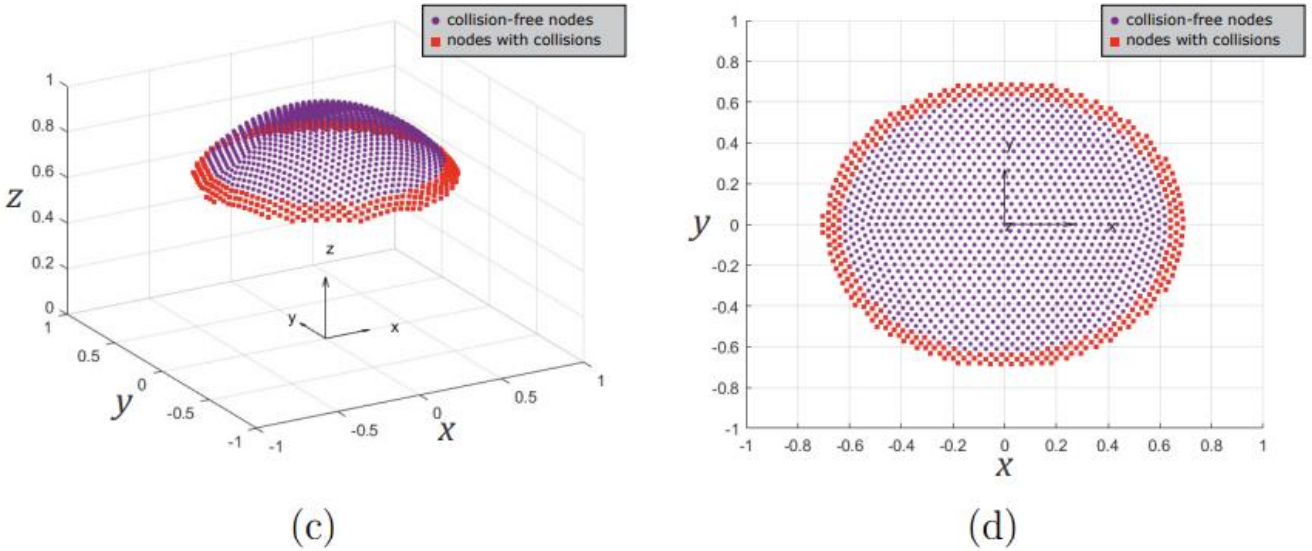

Fig. 35: Test nodes with detected link collisions

Motion Planning

Cartesian Workspace - Results

- At each test point, rotation of the unit vectors $\mathbf{v}_i$, i = 1, 2, 3, was sampled into 360 instants (δ_σ = 1°), and at each instant, unique input joint positions were calculated using Algorithm 2.

- The obtained Cartesian workspace revealed, that the coaxial SPM under study has a cone of 78° opening with full 360° in torsion. It means that this SPM is capable of infinite rotations of its mobile platform with a maximum of 39° tilt from the z-axis.

Motion Planning

Video Example

This video demonstrates three examples of infinite rotational motion of the coaxial SPM at different locations of its Cartesian workspace, alongside with the generated motion trajectories for its actuators:

1. Central region with 0˚-tilted top mobile platform
2. Middle region with 21.43˚-tilted top mobile platform
3. Edge region with 38.22˚-tilted top mobile platform

Motion Planning

Case Study

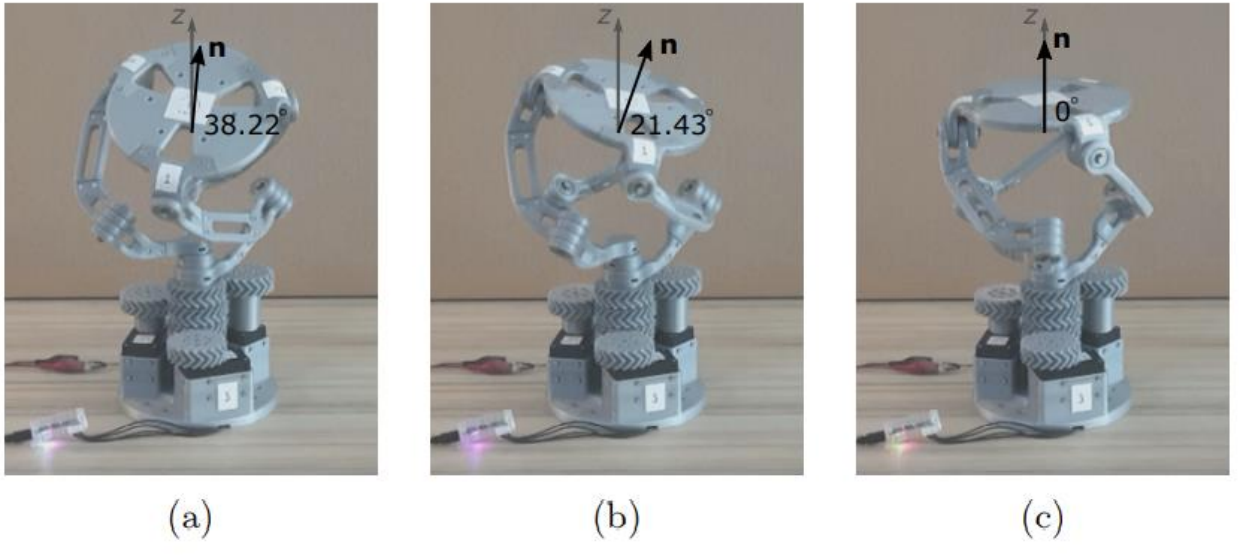

Fig. 36: Case studies of the infinite rotational motion generation of the coaxial SPM prototype

Motion Planning

Case Study

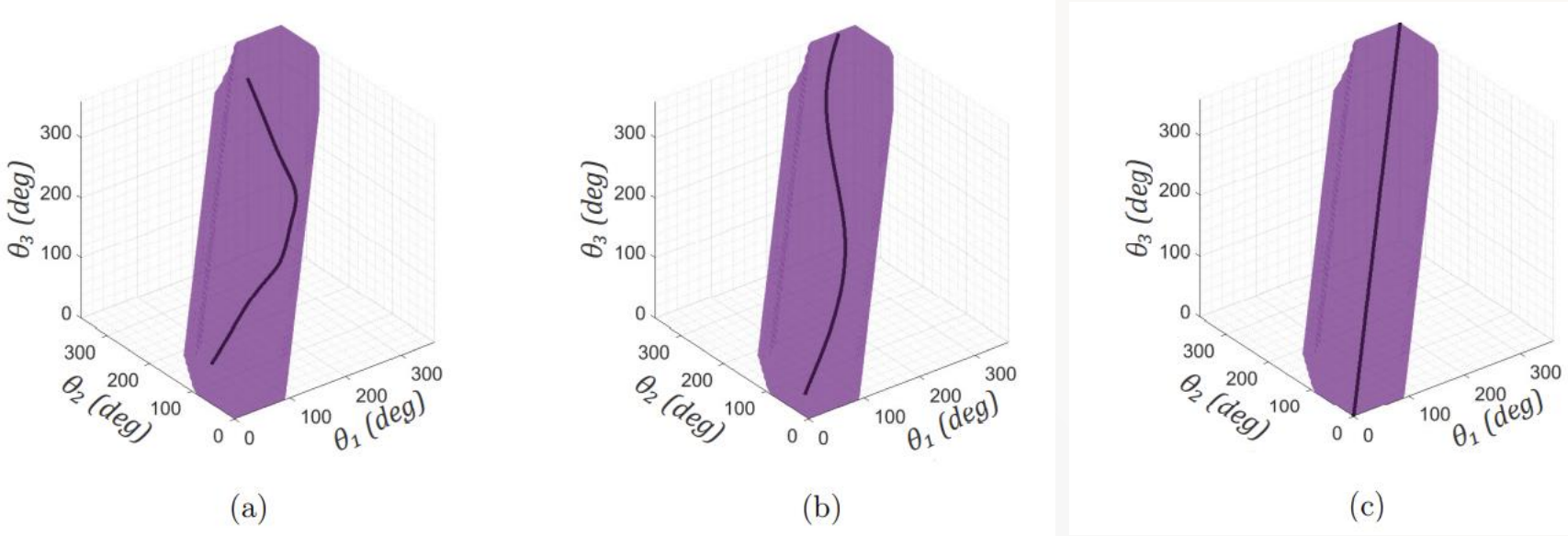

Fig. 37: Generated rotational motion joint trajectories of the coaxial SPM prototype

Motion Planning

Case Study

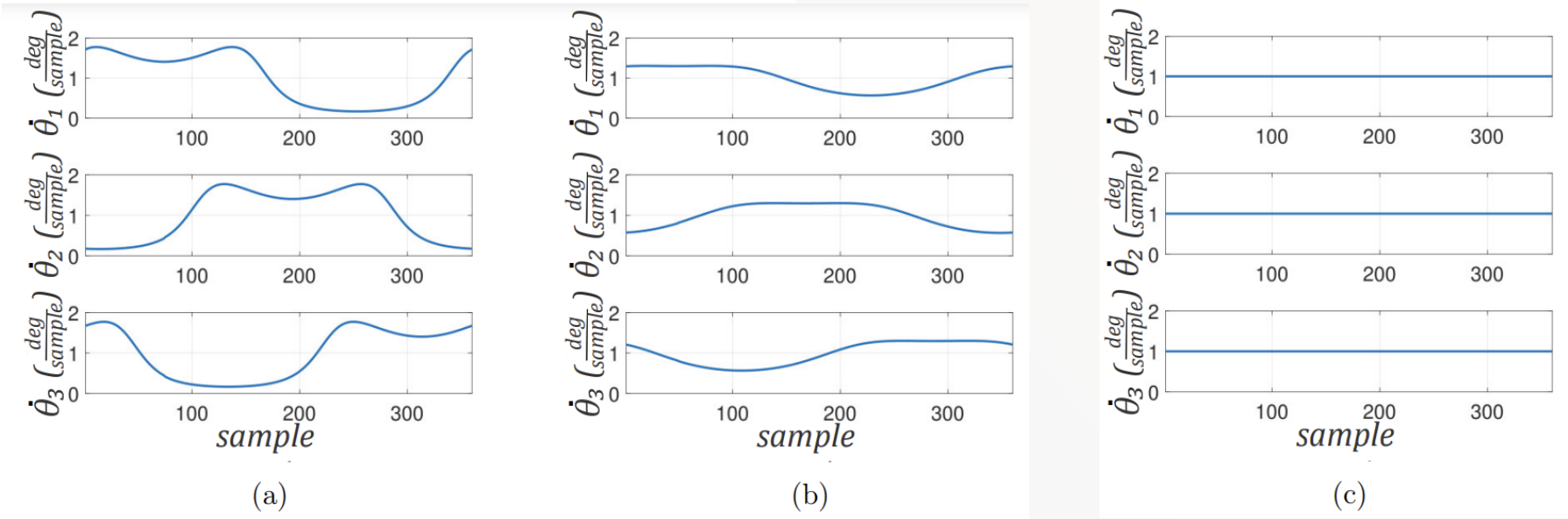

Fig. 38: Evolution of input joint rates of change

Motion Planning

Case Study

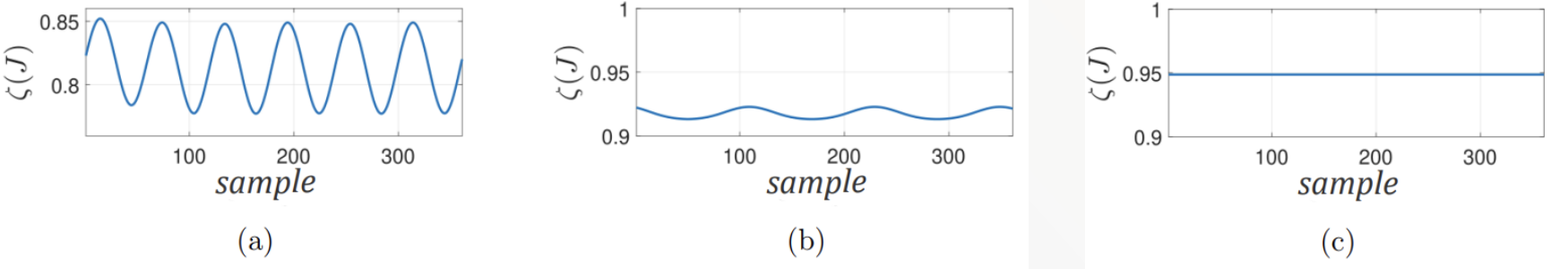

Fig. 39: Evolution of conditioning index $\zeta(\mathbf{J})$

Motion Planning

Journal Paper

Results were published in Mechatronics journal (Elsevier, H-Index 90, Q1), July 2021

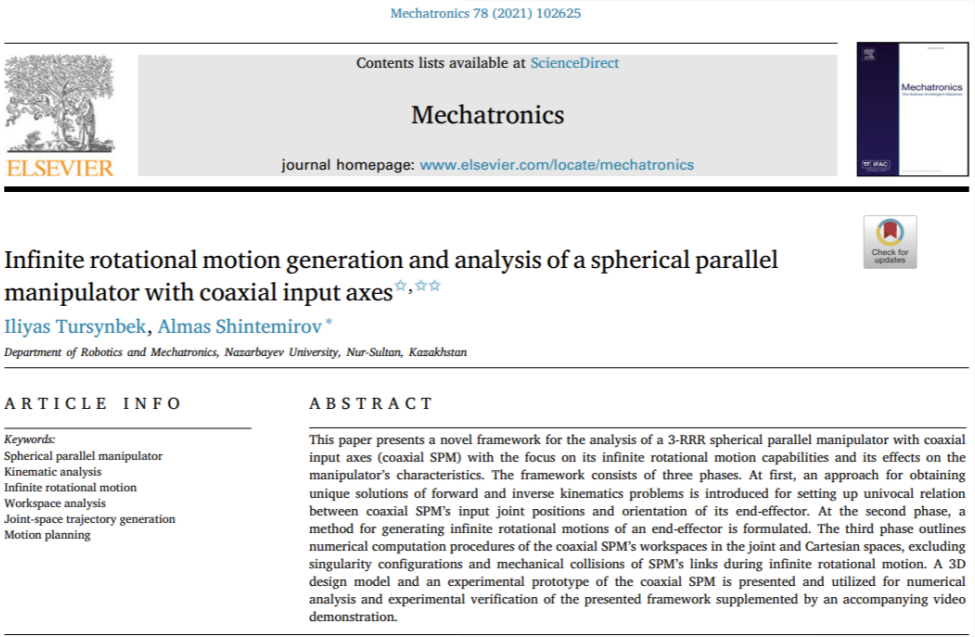

Mechatronics 78 (2021) 102625

Contents lists available at ScienceDirect

Mechatronics

journal homepage: www.elsevier.com/locate/mechatronics

Infinite rotational motion generation and analysis of a spherical parallel manipulator with coaxial input axes☆,☆☆

Iliyas Tursynbek, Almas Shintemirov*

Department of Robotics and Mechatronics, Nazarbayev University, Nur-Sultan, Kazakhstan

ARTICLE INFO

Keywords:
Spherical parallel manipulator
Kinematic analysis
Infinite rotational motion
Workspace analysis
Joint-space trajectory generation
Motion planning

ABSTRACT

This paper presents a novel framework for the analysis of a 3-RRR spherical parallel manipulator with coaxial input axes (coaxial SPM) with the focus on its infinite rotational motion capabilities and its effects on the manipulator's characteristics. The framework consists of three phases. At first, an approach for obtaining unique solutions of forward and inverse kinematics problems is introduced for setting up univocal relation between coaxial SPM's input joint positions and orientation of its end-effector. At the second phase, a method for generating infinite rotational motions of an end-effector is formulated. The third phase outlines numerical computation procedures of the coaxial SPM's workspaces in the joint and Cartesian spaces, excluding singularity configurations and mechanical collisions of SPM's links during infinite rotational motion. A 3D design model and an experimental prototype of the coaxial SPM is presented and utilized for numerical analysis and experimental verification of the presented framework supplemented by an accompanying video demonstration.

Orientation Control

Convex Approximation of the Configuration Space

- To generate optimal trajectories suitable for real-time applications (such as stabilization) using the obtained feasible C-space it is required to obtain its convex approximation.

- In this case, a convex optimization problem can be solved using it.

Orientation Control

Convex Approximation of the Configuration Space

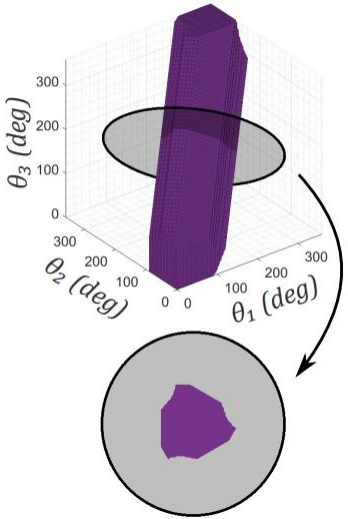

Internal
Convex
Approximation

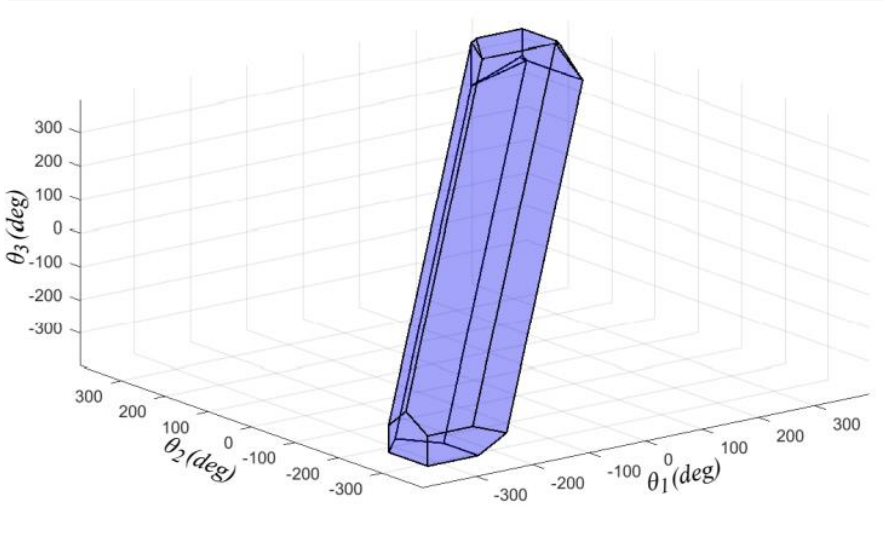

Fig. 40: Internal convex approximation of the feasible C-space

Orientation Control

Convex Approximation of the Configuration Space

Algorithm 6: Convex approximation of the configuration space

Input: $\mathcal{V}$, $\mathcal{F}$, $\boldsymbol{\theta}_{start}$
Output: Set $\mathcal{P}$

```
/* collection of unfeasible areas                                   */
C ← ∅;
for k ← 1 to |F| do
    C ← {C, C_k};
/* initialization of P_temp                                         */
P_temp ← {θ_start};
/* initialization of vertex list P_temp                             */
V_P ← {θ_start};
i ← 0;
while V \ V_P ≠ ∅ do
    i ← i + 1;
    for k ← 1 to |V \ V_P| do
        v_k ← k-th element of V \ V_P;
        /* distance computed as in ()                               */
        d_k ← dist(v_k, P_temp);
    d_min ← min{d_k}_{k=1}^{V\V_P};
    V_N ← {v_j : d_j == d_min};
    for j ← 1 to |V_N| do
        P'_temp = co(P_temp, v_j);
        intersect← false;
        for k ← 1 to |F| do
            if P_temp ∩ C_k ≠ ∅ then
                intersect← true;
                break;
        if intersect == false then
            P_temp ← P'_temp;
            V_P ← V_P ∪ {v_j};
        else
            V ← V \ {v_j};
P ← P_temp;
return P
```

Orientation Control

Convex Approximation of the Configuration Space

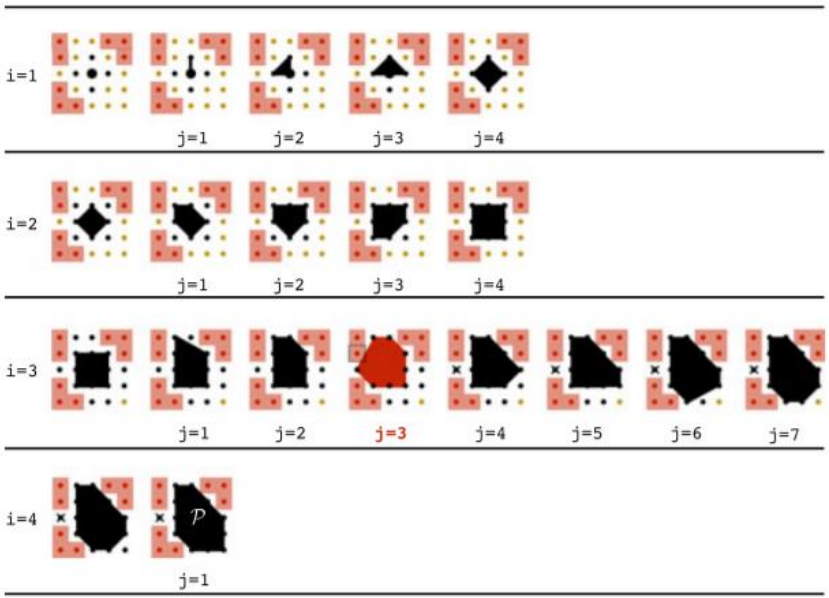

Fig. 41: Convex approximation 2D example [28]

[28] T. Taunyazov, M. Rubagotti, and A. Shintemirov, "Constrained orientation control of a spherical parallel manipulator via online convex optimization," IEEE/ASME Transactions on Mechatronics, vol. 23, no. 1, pp. 252–261, 2017

Orientation Control

Convex Approximation of the Configuration Space - Result

- The initial feasible C-space was modified to include some configuration exceeding the original 3D grid and it was also centered at [0,0,0], i.e., the home configuration.
- Resultant polytope has the H-representation described by A-matrix of the size 43x3, and b-matrix of the size 43x1, i.e., it is described with 43 inequalities.

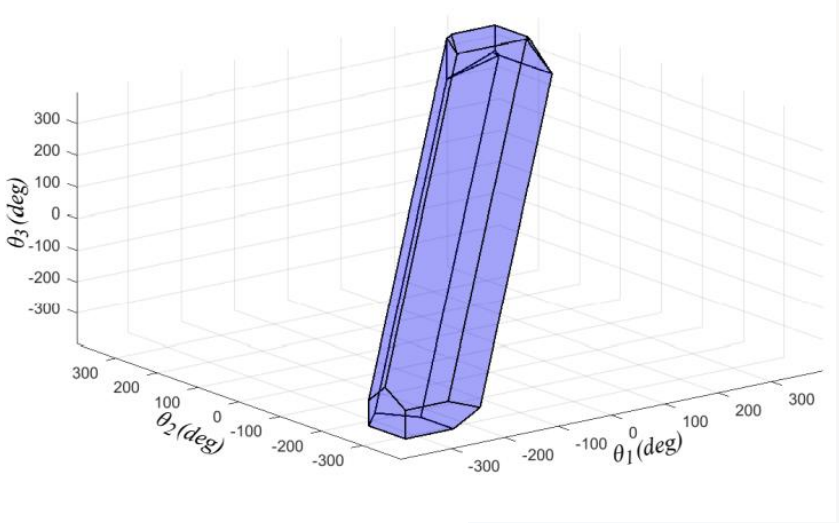

Fig. 40: Internal convex approximation of the feasible C-space

Orientation Control

Target Tracking with Joystick

Fig. 41: Joystick example
COBRA M5

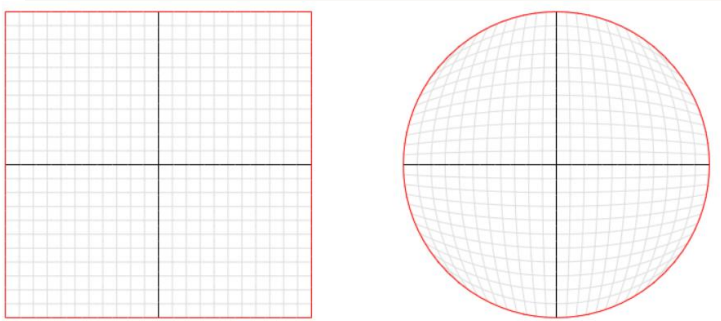

$$(x', y') = \left(x\sqrt{1 - \frac{y^2}{2}}, y\sqrt{1 - \frac{x^2}{2}} \right) \quad (15)$$

$$joystick_z = \sqrt{1 - joystick_x^2 - joystick_y^2} \quad (16)$$

Orientation Control

Target Tracking

- The control command from the joystick is sampled in real-time, the coordinates ($\boldsymbol{q}_{ref}$) are converted (with IK Algorithm 2) to input joints positions to from a reference trajectory $\boldsymbol{\theta}_{ref}$.
- At each command instant, the reference configuration, $\boldsymbol{\theta}_{ref}$, is checked to be within the convex C-space by solving the QP problem each time:

$$\begin{aligned} \boldsymbol{\theta}_{constr} = \arg\min_{\boldsymbol{\theta}} \quad & \|\boldsymbol{\theta} - \boldsymbol{\theta}_{ref}\|_2^2 \\ \text{s.t.} \quad & \mathbf{A}_p\boldsymbol{\theta} \leq \mathbf{b}_p \end{aligned} \tag{17}$$

where $\boldsymbol{A_p\theta} \leq \boldsymbol{b_p}$ is the H-representation of $\mathcal{P}_{\text{temp}}$.

- CVXGEN toolbox (by S. Boyd) for convex optimization can be used. CVXGEN automatically creates library-free C code for a custom, high-speed solver. https://cvxgen.com/

Orientation Control

Target Tracking

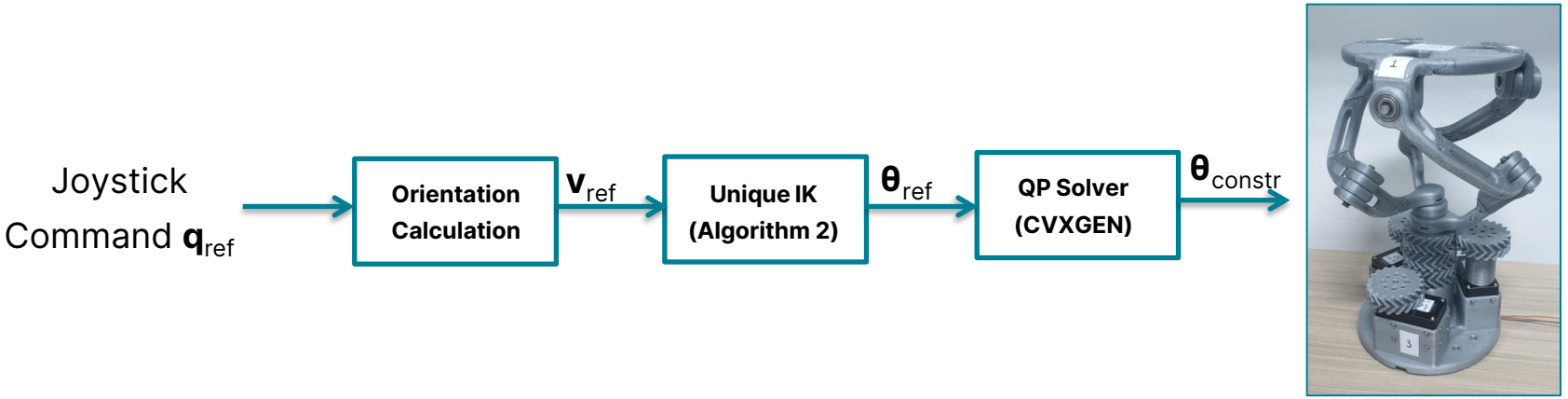

Orientation Control

Target Tracking – Simulation Example

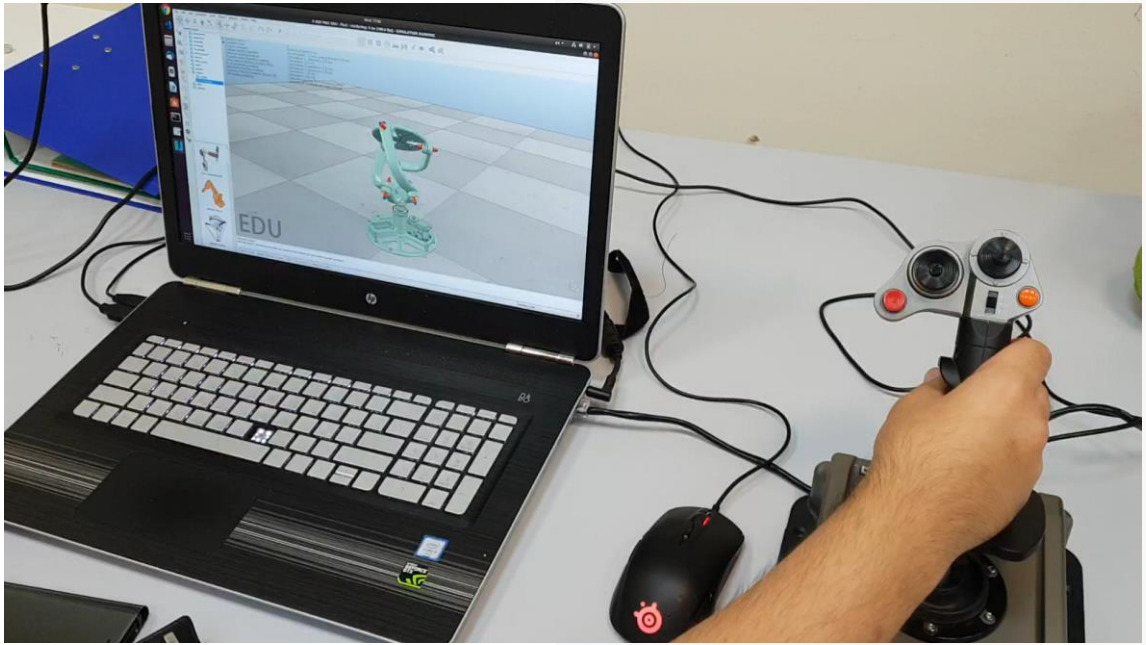

Orientation Control

Target Tracking – Prototype Example with no Roll-Rotation

Orientation Control

Target Tracking – Prototype Example with Roll-Rotation

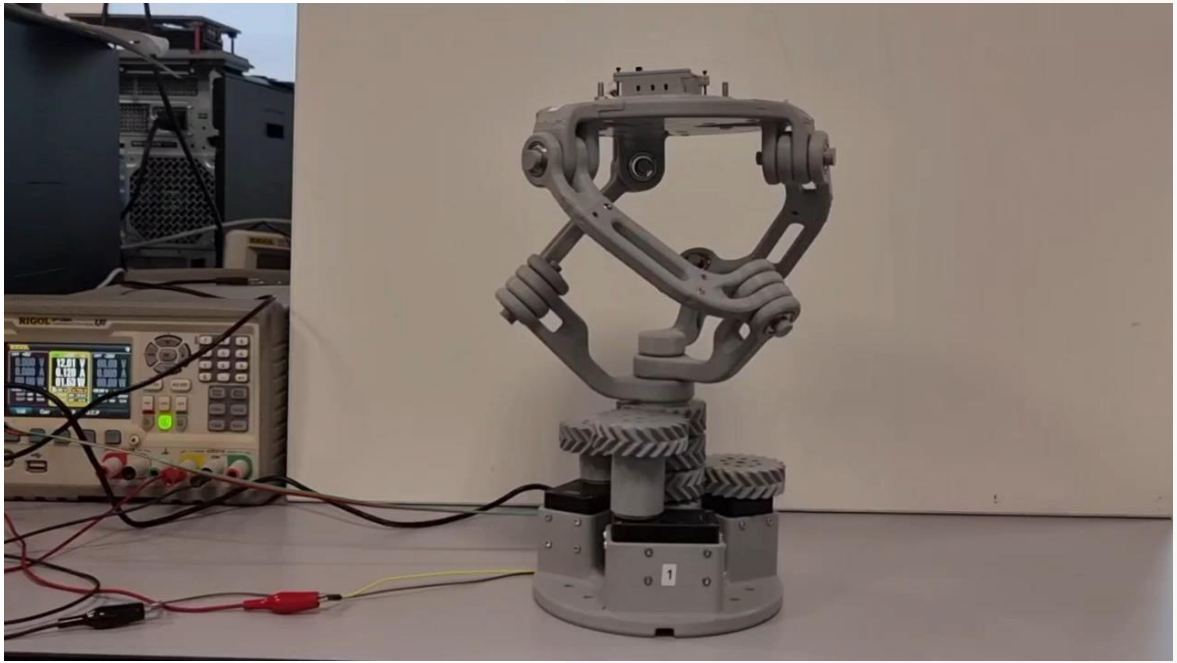

Orientation Control

Target Tracking – Prototype Example with Roll-Rotation

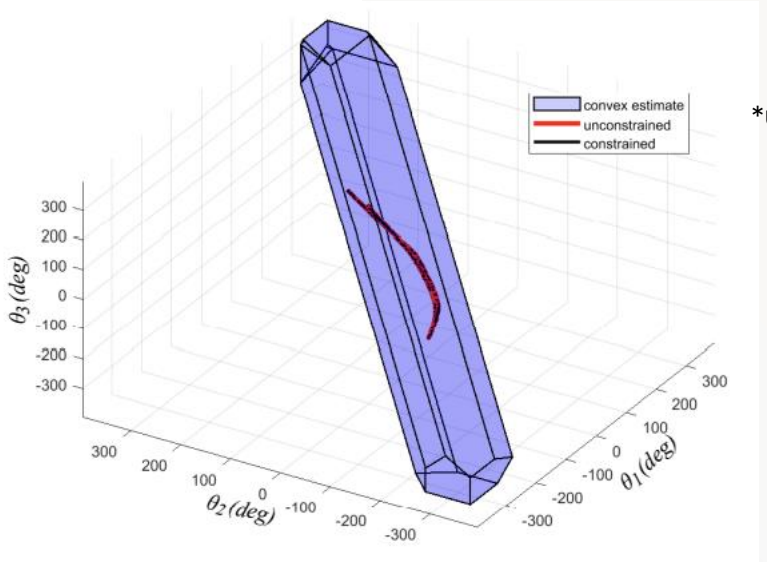

*unconstrained as obtained from the IMU on the mobile platform

Fig. 42: Trajectory for example motion (full-view)

Orientation Control

Target Tracking – Prototype Example with Roll-Rotation

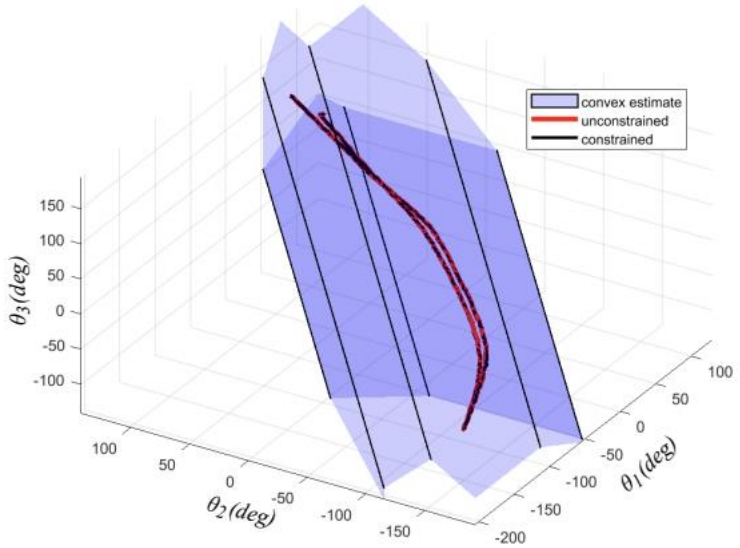

*unconstrained as obtained from the IMU on the mobile platform

Fig. 43: Trajectory for example motion (zoomed-in view)

Orientation Control

Target Tracking

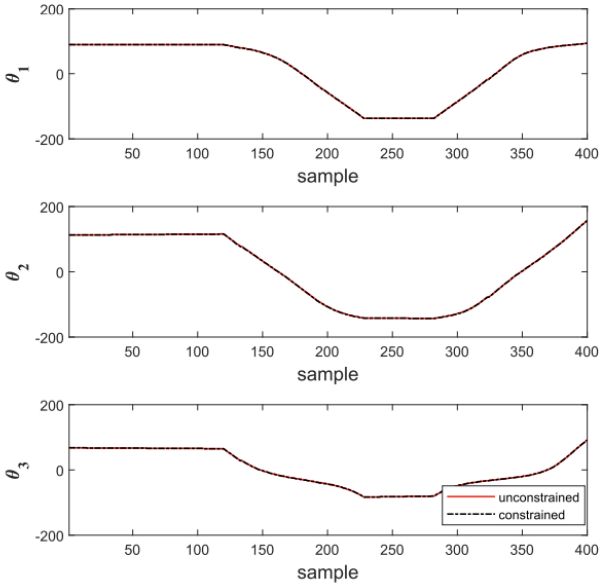

Fig. 44: Resultant trajectory, θ_{constr} (black) vs. trajectory as calculated from the IMU sensor data q_{mp} (red)

Orientation Control

Target Tracking – another control device

Fig. 45: RSX-UM7 IMU Orientation Sensor

Orientation Control

Object Stabilization

- The orientation of the base is provided in the form of an orientation quaternion at each sampling instant, q_{base}. The resulting quaternion for calculation of input joint position to achieve stabilization of the mobile platform is calculated as:

$$\mathbf{q} = \mathbf{q}_{base}^{-1} \times \mathbf{q}_{ref}$$

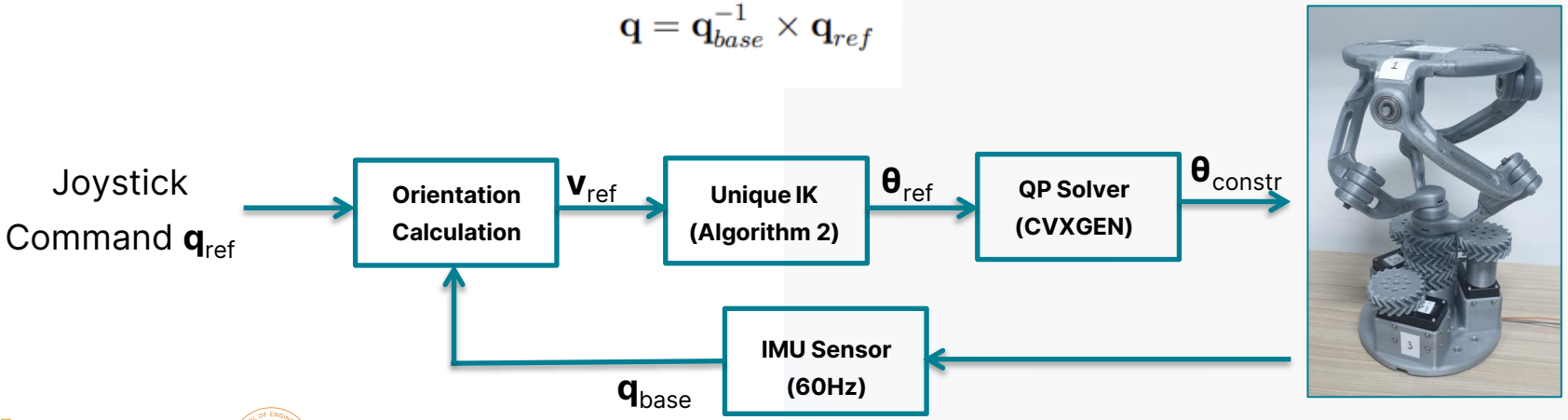

Orientation Control

Object Stabilization

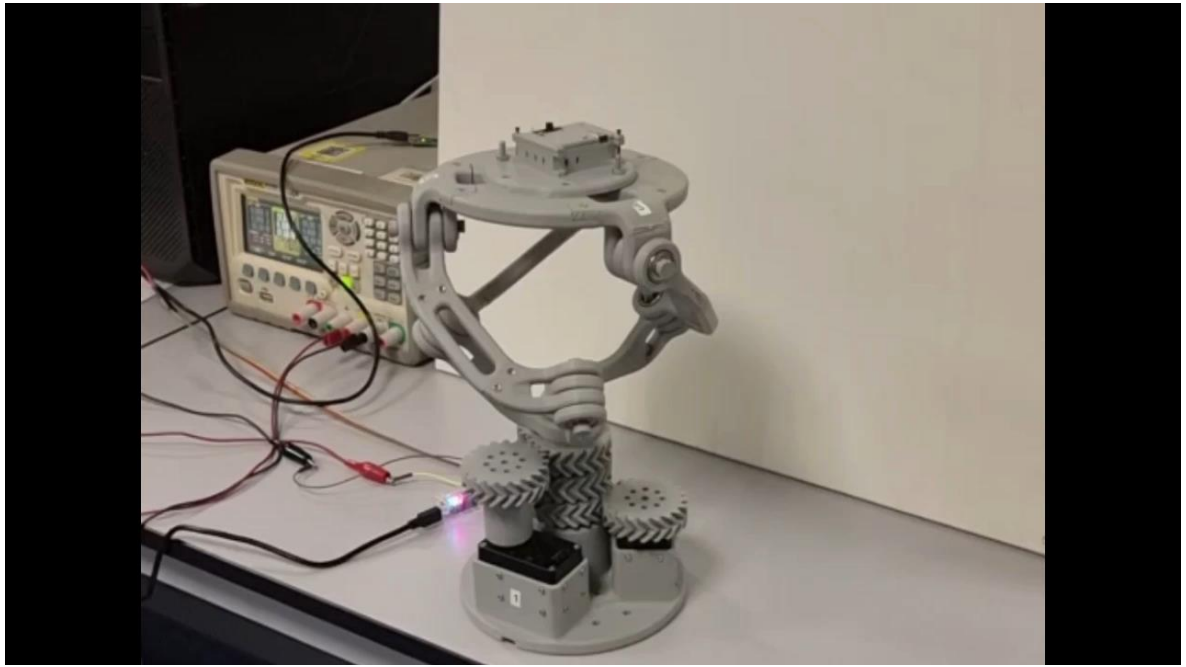

Control is implemented in ROS framework with Python scripting.

ROS allows to integrate Dynamixels, joystick, IMUs, QP solver easily together.

ROS

Orientation Control

Object Stabilization

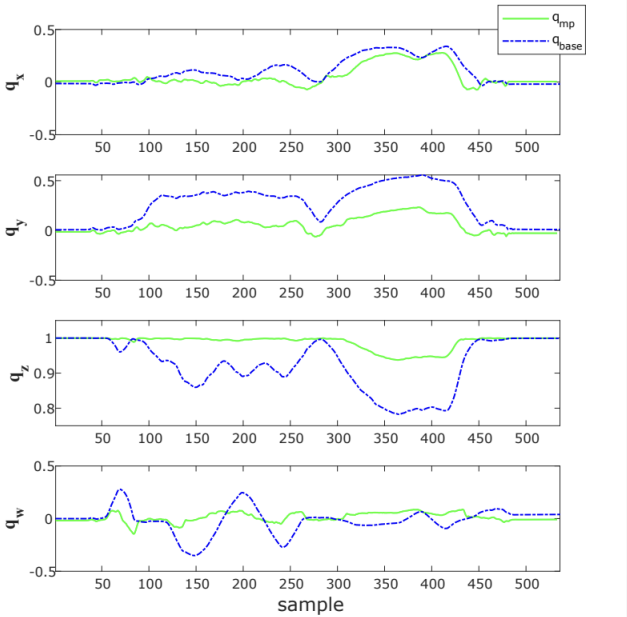

Fig. 46: Orientations of the coaxial SPM's mobile platform, q_{mp}, and base platform q_{base}

Orientation Control

Object Stabilization

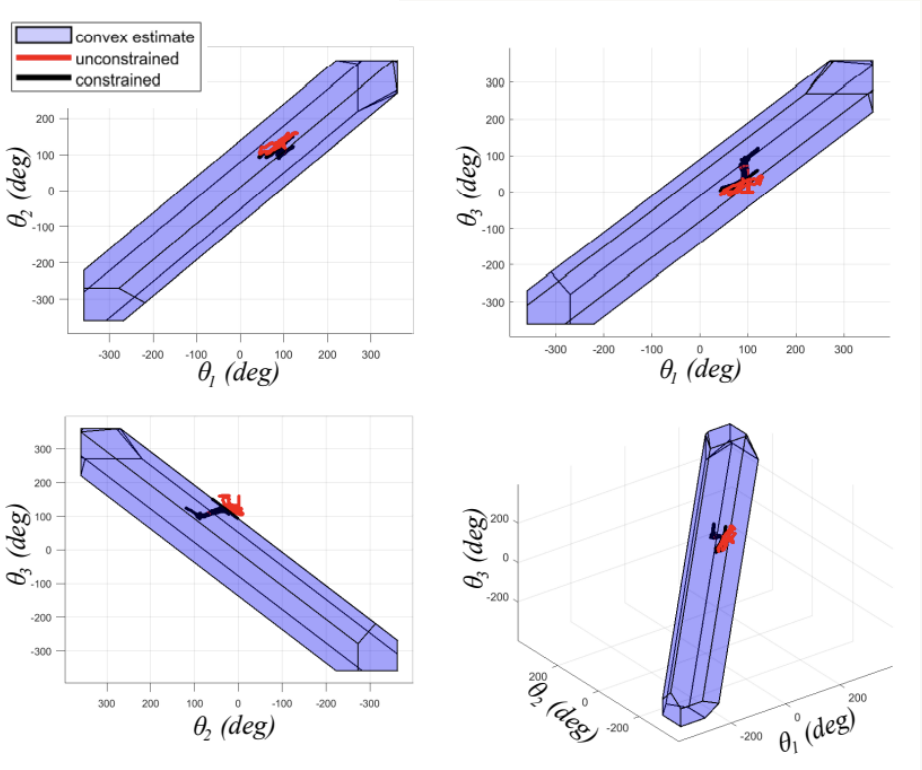

Fig. 47: Trajectory for motion from different view angles

Orientation Control

Object Stabilization

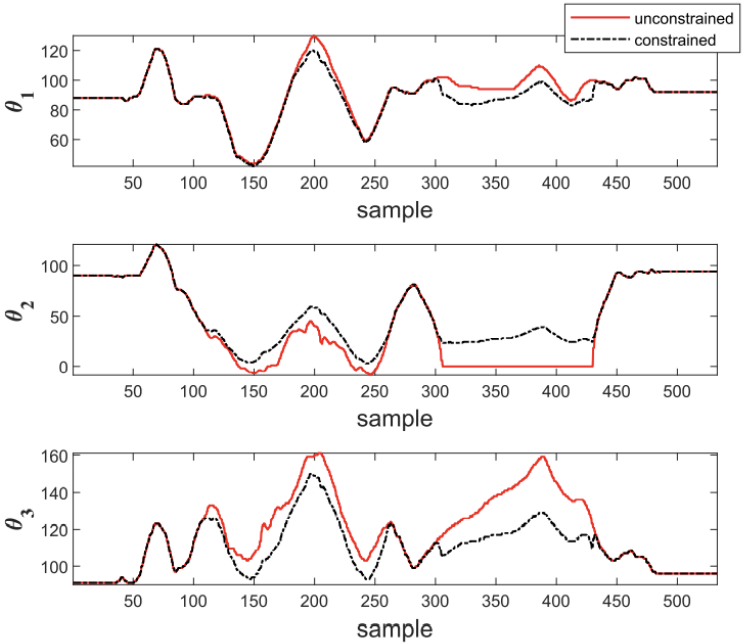

Fig. 48: Constrained input joint positions $\boldsymbol{\theta}_{constr}$ as calculated from $\boldsymbol{q}$

Conclusion

Summary of the Results and Review of Contributions

- In this thesis, it was investigated if motion control platforms can be developed based on the coaxial SPM with capabilities to infinitely rotate its mobile platform and achieve target tracking and object stabilization.
- All tasks for the coaxial SPM-based motion control platform were achieved and experimentally demonstrated.
- A working prototype capable or target tracking and object stabilization was obtained.

Conclusion

Limitations of the Reported Research

- Accuracy of the manufactured prototype is low since it was 3D printed. Manufacture it using CNC milling with metal. However, that would increase the cost of the prototype, and at the current stage having a 3D printed version is enough, since some design modifications can be introduced easier and faster.
- Another issue is the poor accuracy of the IMU sensor used (UM7 from CHRobotics). The measurements provided were not stable, and the effect of sensor drifting was present.
- Since a numerical approach was used in obtaining the configuration space, its representation cannot be the most precise one. A higher sampling of the tested 3D space would be desirable, however, it would come at the expense of the increased computation time.

Conclusion

Recommendations for Future Research

- Optimization of the manipulator’s design to obtain a larger configuration space.
- Velocity control for the actuators can be investigated for the generation of infinite rotational motions as it was observed that there is some dependency between such rotations and input joint position rates.
- Dynamic analysis can also be conducted to be incorporated into the overall stabilization control framework, taking the effect of external forces into effect.

List of Publications

1. **Tursynbek I**, Niyetkaliyev A, Shintemirov A. *Computation of unique kinematic solutions of a spherical parallel manipulator with coaxial input shafts*. In 2019 IEEE 15th International Conference on Automation Science and Engineering (CASE) 2019 Aug 22 (pp. 1524-1531). IEEE.
2. **Tursynbek I**, Shintemirov A. *Infinite torsional motion generation of a spherical parallel manipulator with coaxial input axes*. In 2020 IEEE/ASME International Conference on Advanced Intelligent Mechatronics (AIM) 2020 Jul 6 (pp. 1780-1785). IEEE.
3. **Tursynbek I**, Shintemirov A*. Modeling and simulation of spherical parallel manipulators in CoppeliaSim (V-REP) robot simulator software*. In 2020 International Conference Nonlinearity, Information and Robotics (NIR) 2020 Dec 3 (pp. 1-6). IEEE.
4. **Tursynbek I**, Shintemirov A. *Infinite rotational motion generation and analysis of a spherical parallel manipulator with coaxial input axes*. Mechatronics. 2021 Oct 1; 78:102625.
5. *Orientation and trajectory tracking control of a coaxial spherical parallel manipulator*. **In-progress**

Acknowledgements

- I would like to thank my supervisory team for their support and guidance.
- I am also thankful to the Department of Robotics, SEDS, NU and Alaris Lab for providing support financially and for the amazing facilities.
- I am also grateful to my colleagues, friends, and students for their moral support.
- Thanks to my parents and relatives. Their belief in me has kept my spirits and motivation high.
- Lastly, I would also like to express my sincere gratitude to the defense committee members for their time and expertise.

IEEE CASE 2019

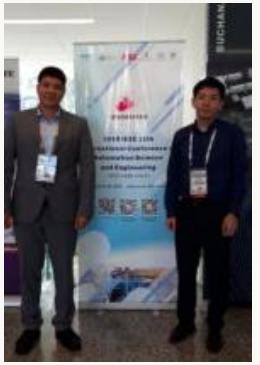

Summer Schools:
PKM2018, SIMERO2019

List of References

[1] W. Shang, S. Cong, and Y. Zhang, “Nonlinear friction compensation of a 2-dof planar parallel manipulator,” Mechatronics, vol. 18, no. 7, pp. 340–346, 2008.
[2] K. Elashry, and R. Glynn, “An approach to automated construction using adaptive programing,” In Robotic Fabrication in Architecture, Art and Design 2014, pp. 51-66. Springer, Cham, 2014.
[3] C. M. Gosselin, E. St. Pierre, and M. Gagne, “On the development of the Agile Eye,” IEEE Robotics & Automation Magazine, vol. 3, no. 4, pp. 29–37, 1996.
[4] K. Al-Widyan, X. Q. Ma, and J. Angeles, “The robust design of parallel spherical robots,” Mechanism and Machine Theory, vol. 46, no. 3, pp. 335–343, 2011.
[5] H. Asada and J. Granito, “Kinematic and static characterization of wrist joints and their optimal design,” in Proceedings of the 1985 IEEE International Conference on Robotics and Automation (ICRA), pp. 244–250, 1985.
[6] D. J. Cox and D. Tesar, “The dynamic model of a three degree of freedom parallel robotic shoulder module,” in Advanced Robotics: 1989, pp. 475–487, Springer, 1989.
[7] D. Marco, L. Torfason, and D. Tesar, “Computer simulation and design of a three degree-of-freedom shoulder module,” pp. 273–282, 1989.
[8] W. M. Craver, “Structural analysis and design of a three-degree-of-freedom robotic shoulder module,” Master’s thesis, University of Texas, Austin TX, 1989.
[9] R. I. Alizade, N. R. Tagiyev, and J. Duffy, “A forward and reverse displacement analysis of an in-parallel spherical manipulator,” Mechanism and Machine Theory, vol. 29, no. 1, pp. 125–137, 1994.
[10] C. M. Gosselin and J. Angeles, “The optimum kinematic design of a spherical three-degree-of-freedom parallel manipulator,” Journal of Mechanisms, Transmissions, and Automation in Design, vol. 111, no. 2, pp. 202–207, 1989.

List of References

[11] C. M. Gosselin, J. Sefrioui, and M. J. Richard, “On the direct kinematics of spherical three-degree-of-freedom parallel manipulators with a coplanar platform,” Journal of Mechanical Design, vol. 116, no. 2, pp. 587–593, 1994.
[12] C. M. Gosselin, J. Sefrioui, and M. J. Richard, “On the direct kinematics of spherical three-degree-of-freedom parallel manipulators of general architecture,” Journal of Mechanical Design, vol. 116, no. 2, pp. 594–598, 1994.
[13] C. M. Gosselin and J.-F. Hamel, “The Agile Eye: a high-performance three-degree-of-freedom camera-orienting device,” in Proceedings of the 1994 IEEE International Conference on Robotics and Automation (ICRA), pp. 781–786, 1994.
[14] X. Kong and C. M. Gosselin, “A formula that produces a unique solution to the forward displacement analysis of a quadratic spherical parallel manipulator: the Agile Eye,” Journal of Mechanisms and Robotics, vol. 2, no. 4, 2009.
[15] J. Angeles, A. Morozov, L. Slutski, O. Navarro, and L. Jabre, “The modular design of a long-reach, 11-axis manipulator,” in Romansy 13, pp. 225–233, Springer, 2000.
[16] L. Birglen, C. M. Gosselin, N. Pouliot, B. Monsarrat, and T. Laliberte, “SHaDe, a new 3-DOF haptic device,” IEEE Transactions on Robotics and Automation, vol. 18, no. 2, pp. 166–175, 2002.
[17] H. Saafi, M. A. Laribi, and S. Zeghloul, “Optimal haptic control of a redundant 3-RRR spherical parallel manipulator,” in 2015 IEEE/RSJ International Conference on Intelligent Robots and Systems (IROS), pp. 2591–2596, 2015.
[18] P. Vischer and R. Clavel, “Kinematic calibration of the parallel Argos mechanism,” Robotica, vol. 18, no. 6, pp. 589–599, 2000.
[19] Gosselin, Clément M., and Jing Wang. "Singularity loci of a special class of spherical three-degree-of-freedom parallel mechanisms with revolute actuators." The International Journal of Robotics Research 21, no. 7 (2002): 649-659.
[20] M. E. Rosheim and G. F. Sauter, “New high-angulation omni-directional sensor mount,” in SPIE Free-Space Laser Communication and Laser Imagngg II, pp. 163–174, 2002.

List of References

[21] S. Bai, “Optimum design of spherical parallel manipulators for a prescribed workspace,” Mechanism and Machine Theory, vol. 45, no. 2, pp. 200–211, 2010.
[22] B. Sudki, M. Lauria, and F. Noca, “Robotic penguin-like propulsor with novel spherical joint,” in Proceedings of the Third International Symposium on Marine Propulsors, 2013.
[23] J. Noh, J. Lee, W. Yang, and S. Lee, “Design of a concentrically stacked modular actuator with forced air cooling for multi-DOF robotic systems,” Energies, vol. 11, no. 11, 2018.
[24] G. Wu, “Parameter-excited instabilities of a 2UPU-RUR-RPS spherical parallel manipulator with a driven universal joint,” Journal of Mechanical Design, vol. 140, no. 9, 2018.
[25] C. M. Gosselin and E. Lavoie, “On the kinematic design of spherical three-degree-of-freedom parallel manipulators,” The International Journal of Robotics Research, vol. 12, no. 4, pp. 394–402, 1993.
[26] S. Gottschalk, M. C. Lin, and D. Manocha, “OBBTree: A Hierarchical Structure for Rapid Interference Detection,” in Proceedings of the 23rd annual conference on Computer graphics and interactive techniques – ACM SIGGRAPH, pp. 171–180, 1996.
[27] C. M. Gosselin and J. Angeles, “Singularity analysis of closed-loop kinematic chains,” IEEE Transactions on Robotics and Automation, vol. 6, no. 3, pp. 281–290, 1990.
[28] T. Taunyazov, M. Rubagotti, and A. Shintemirov, “Constrained orientation control of a spherical parallel manipulator via online convex optimization,” IEEE/ASME Transactions on Mechatronics, vol. 23, no. 1, pp. 252–261, 2017

Thank you
for your attention!

NAZARBAYEV
UNIVERSITY